ELSEVIER

Tectonophysics 292 (1998) 229–254

TECTONOPHYSICS

The role of pre-existing thrust faults and topography on the styles of extension in the Gran Sasso range (central Italy)

Nicola D'Agostino [a,*], Nicolas Chamot-Rooke [b], Renato Funiciello [a], Laurent Jolivet [c], Fabio Speranza [a]

[a] *Dipartimento di Scienze Geologiche, Università degli Studi di Roma 3, Largo S. Leonardo Murialdo, 1, 00146 Roma, Italy*
[b] *Laboratoire de Géologie, CNRS–URA 1316, Ecole Normale Supérieure, 24 rue Lhomond, 75231 Paris Cedex 05, France*
[c] *Départment de Géotectonique, Université P. and M. Curie, Case 129-T 26-E1-4 Place Jussieu, F75252 Paris Cedex 05, France*

Received 27 March 1997; accepted 9 February 1998

Abstract

Structural analysis and field mapping together with simple geometrical and flexural elastic models, document that two styles of Quaternary extensional tectonics characterized the Gran Sasso range (central Apennines, Italy). In the western part of the range, extension took place on 10–15-km-long range-front normal faults with associated 600–1000-m-high escarpments showing evidence of Late Glacial–Holocene activity. This topography has been reproduced with a thin elastic plate subjected to the isostatic forces induced by the movement along high-angle (55°–65°) planar normal faults. In the eastern part of the belt extension occurred on shallow-dipping normal faults (30°–35°) which reactivated progressively deeper pre-existing thrusts. In this area antithetic 'domino' faults formed to accommodate the mechanical adjustment of the hanging-wall over a variably dipping major fault surface. The eastward increase in shortening, due to the earlier compressional phase, documented in the Gran Sasso belt by previous authors, accounts for the more developed zones of weakness and high topographic relief in the eastern sector. This setting could explain the different styles of extension and the more advanced northeastern limit of normal faulting in the eastern sector. This work suggests that normal faults can originate either with low- or high-angle geometry in the upper crust according to the pre-existing tectonic setting and that topography could be important in controlling the geometry and pattern of migrating normal faulting.

Keywords: extensional tectonics; Quaternary; thrust faults; topography; Apennines

1. Introduction

Pre-existing faults and topography may control the styles of extensional faulting especially in mountain chains undergoing post-orogenic extension. Geometric relationships between normal and thrust faults are usually described as branching on décollement levels (Bally et al., 1966; Royse et al., 1975), reactivation of ramps (Petersen et al., 1984; Smith and Bruhn, 1984) or cross-cutting of thrusts by normal faults (Wernicke et al., 1985; Powell and Williams, 1989). Mechanical models based on the Mohr–Coulomb criterion (Sibson, 1985; Ivins et al., 1990; Huyghe and Mugnier, 1992), evidence from earthquakes focal mechanisms (Jackson and White,

* Corresponding author. Fax: +39 6548 88201; E-mail: ndagosti@uniroma3.it

0040-1951/98/$19.00
PII S0040-1951(98)00070-5

1989; Doser, 1987) and analogue models (Faccenna et al., 1995) put some constraints on the geometric conditions allowing extensional reactivation of thrust faults in the upper brittle crust. Topography also influences the state of stress (Fleitout and Froidevaux, 1982; Royden and Burchfiel, 1987) generating extensional regimes in elevated terrains. The styles of extension can thus change very rapidly in the same area, depending on the pre-existing structural and topographic setting.

The Apennines thrust belt formed after the late Tortonian, contemporaneously with back-arc accretion in the Tyrrhenian Sea (Malinverno and Ryan, 1986; Patacca et al., 1990). Progressively eastern domains of the Adriatic foreland were affected by shortening and thrusting followed by extensional tectonics (Elter et al., 1975; Bally et al., 1986; Keller et al., 1994). Today, the eastern limit of normal faulting follows the topographic divide of the Apennines (Fig. 1). The migrating extensional front reached this position in the Early Pleistocene. Active SW–NE extension is also evidenced by the pattern of seismicity observed in the Italian Peninsula (Anderson and Jackson, 1987). At the regional scale the system of nor-

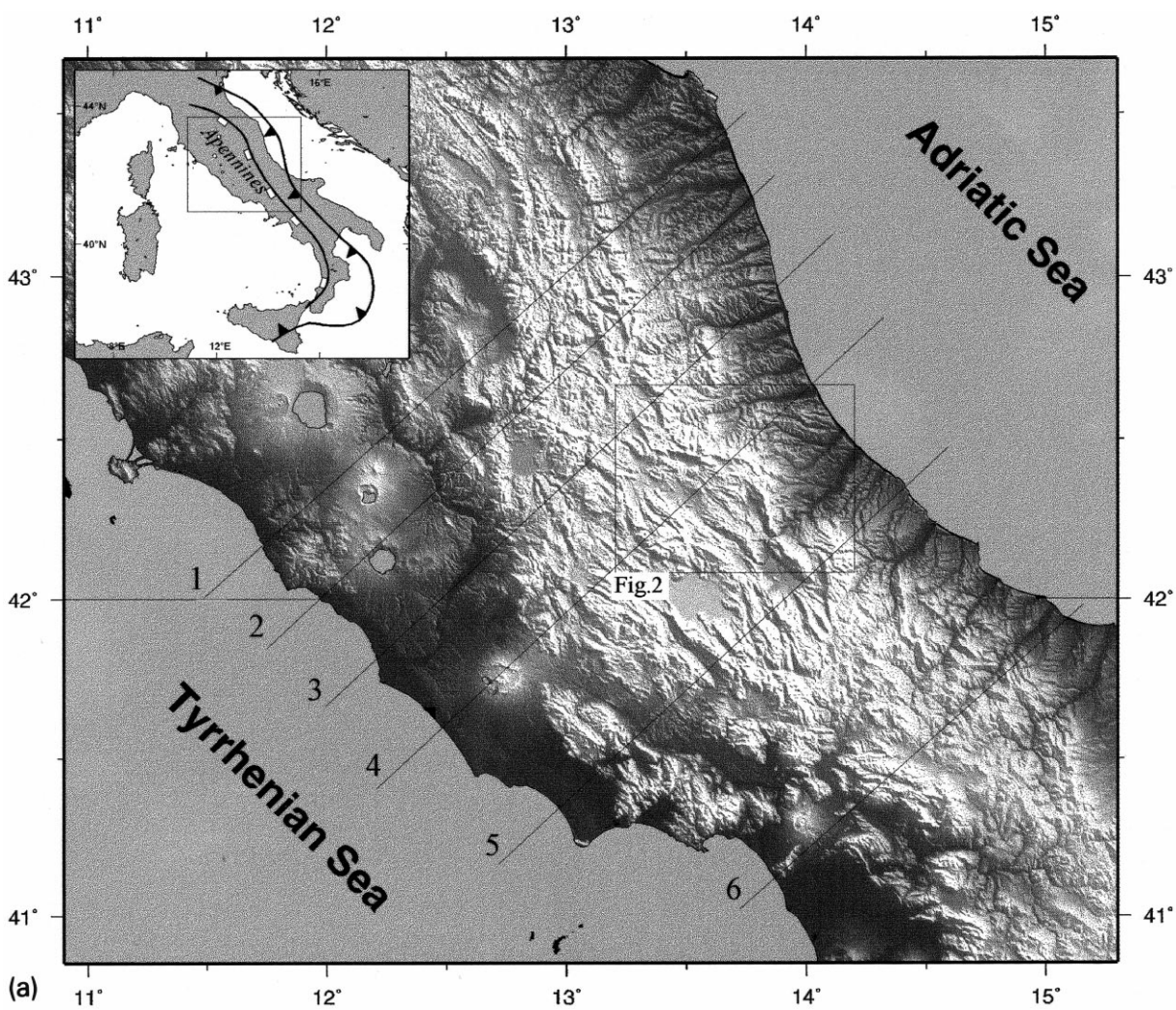

Fig. 1. (a) Shaded relief map of central Italy and (b) topographic cross-sections. The inset outlines the area showed in Figs. 2 and 3. The topographic cross-sections show that significant normal faulting begins immediately behind the topographic crest of the Apennines.

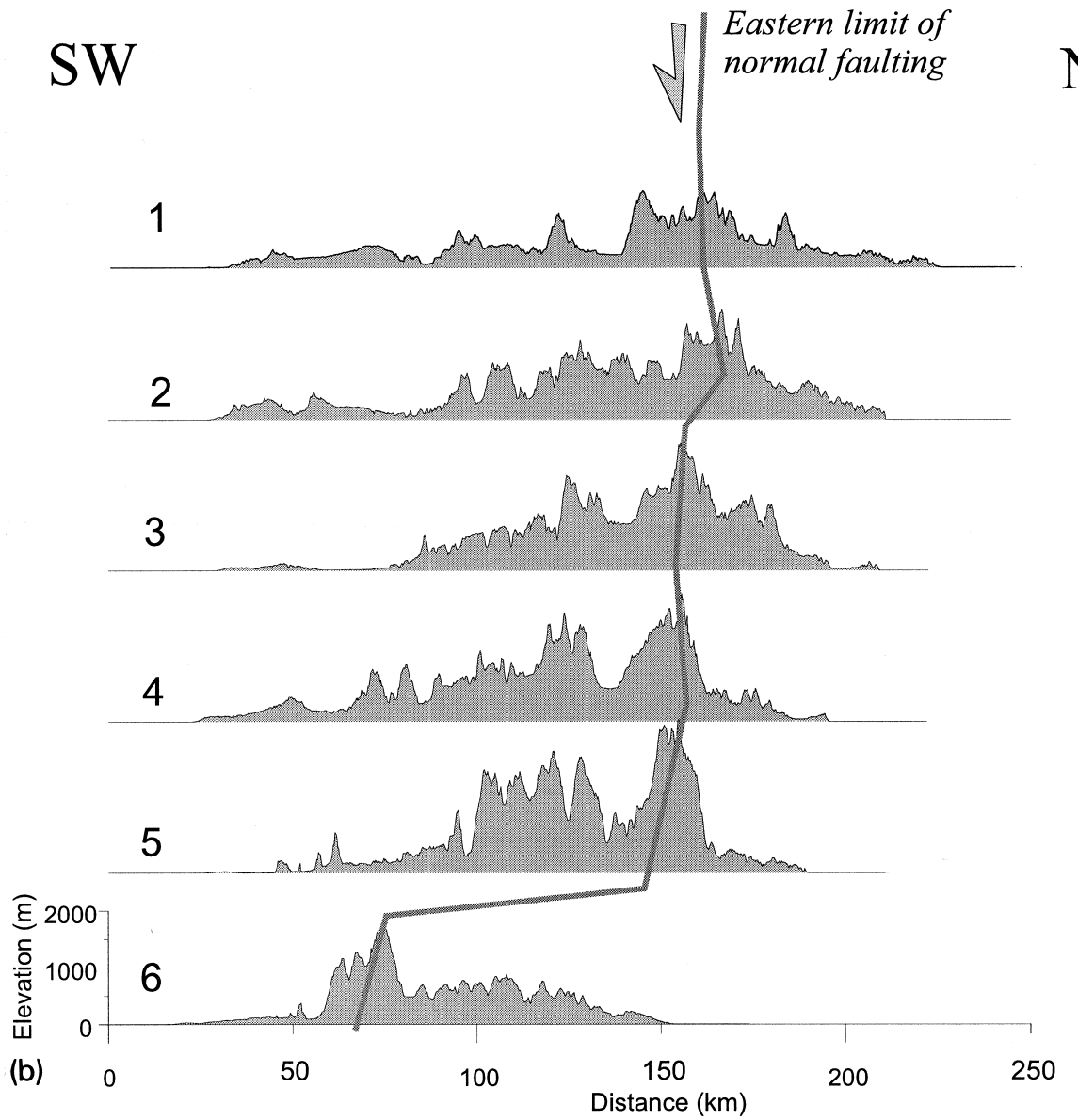

Fig. 1 (continued).

mal faults runs NW–SE, almost parallel to the frontal Apenninic thrust system. In the Gran Sasso area the regional trend of normal faults is locally deflected assuming E–W and N–S directions, following the arcuate shape of the thrust sheet. This pattern gives the opportunity to study the role of pre-existing thrust faults and topography on the styles of extension.

In this paper we present new data concerning the structural setting of extensional faults in the Gran Sasso range. We focus in particular on (1) the role of pre-existing faults and topography in controlling normal faults geometry and kinematics, and (2) on the modes of outer migration of normal faulting. Geometric and simple thin elastic plate models put some constraints on the geometry and the kinematic evolution of the normal faults.

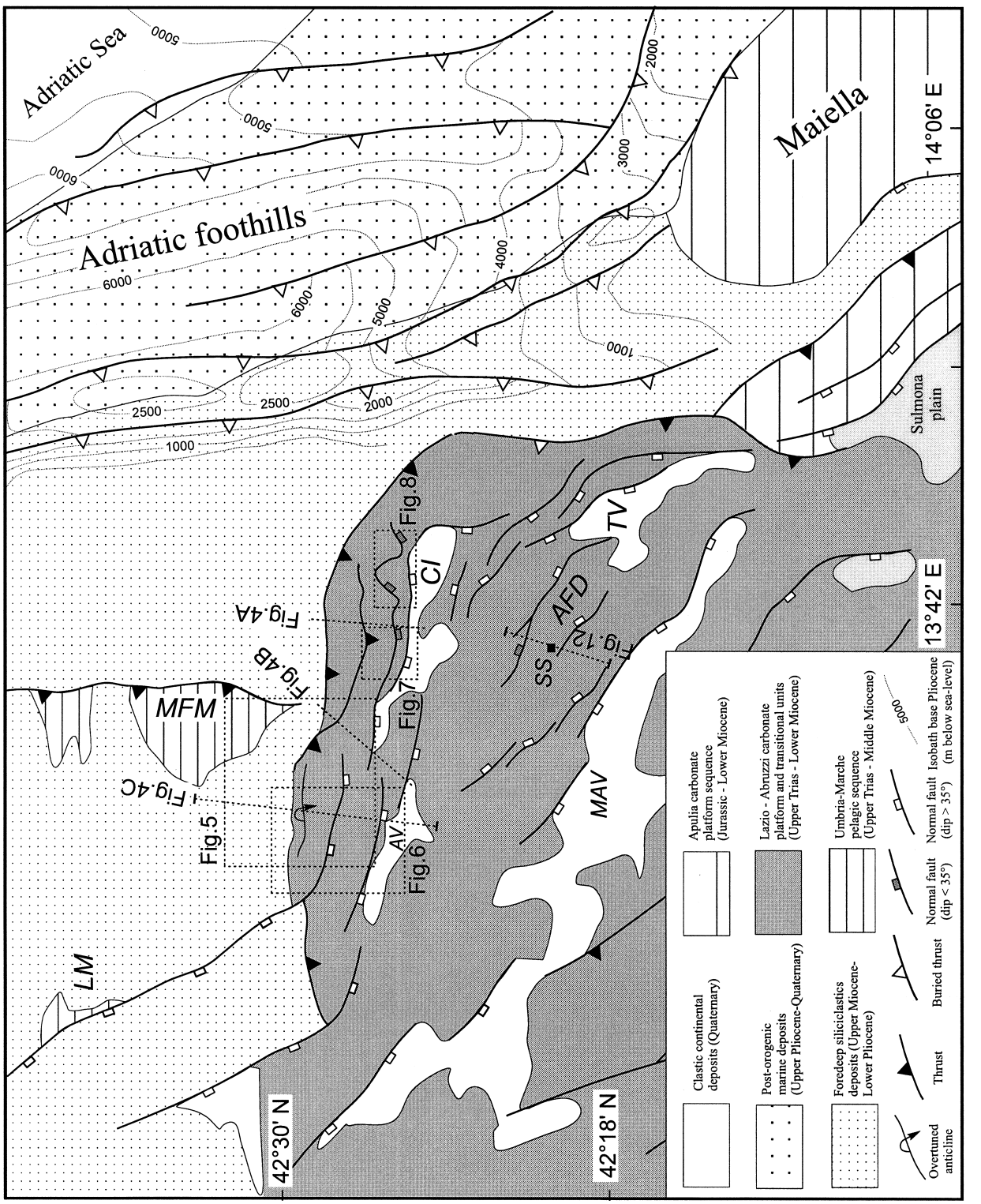
Adriatic Sea
Adriatic foothills
Maiella
Sulmona plain
14°06' E
13°42' E
42°30' N
42°18' N
LM
MFM
AV
CI
AFD
TV
MAV
SS
Fig.4A
Fig.4B
Fig.4C
Fig.5
Fig.6
Fig.7
Fig.8
Fig.12
Clastic continental deposits (Quaternary)
Post-orogenic marine deposits (Upper Pliocene-Quaternary)
Foredeep siliciclastics deposits (Upper Miocene-Lower Pliocene)
Apulia carbonate platform sequence (Jurassic - Lower Miocene)
Lazio - Abruzzi carbonate platform and transitional units (Upper Trias - Lower Miocene)
Umbria-Marche pelagic sequence (Upper Trias - Middle Miocene)
Overturned anticline
Thrust
Buried thrust
Normal fault (dip < 35°)
Normal fault (dip > 35°)
Isobath base Pliocene (m below sea-level)

A clearer definition of the extensional tectonics in this area is important in order to provide insights into: (1) upper crustal normal fault geometry in an intra-continental extensional setting containing pre-existing zones of weakness and topographic relief; (2) the modes of extensional tectonics in orogenic belts where normal faulting underwent spatial and temporal migration in a previously shortened domain; (3) the geometrical and kinematic relationships between thrusts and normal faults during the Quaternary tectonic evolution of the central Apennines.

2. Geological setting

The Gran Sasso range (Fig. 2) is one of the major morphological and structural features of the central Apennines (Parotto and Praturlon, 1975). It has the highest altitude in the belt (2912 m at Corno Grande) and forms an E–W to N–S trending arcuate thrust belt (Gran Sasso Thrust Belt, GSTB). Several studies have focused on the compression-related structural features describing the out-of-sequence character of the GSTB (Ghisetti and Vezzani, 1986, 1991).

In the GSTB the most easterly normal faults of the central Apennines represent the breakaway fault system of the Tyrrhenian–Apennines extensional domain. Despite evidence of important normal faulting, few studies have focused on the Quaternary extensional tectonics which characterizes the internal part of the range. The GSTB is particularly well suited for a structural study on the influence of pre-existing structures on the development of extensional faulting, as the normal faults developed in (1) a regionally important thrust belt and are (2) the outermost zone of the Apennines extensional domain.

Based on the structural and morphological features of the GSTB extensional area, three different domains are distinguished (Fig. 3). In the western part (Assergi Valley) (a), normal faults dipping 50°–70° to the south, show ~1000-m-high and 10–15-km-long fault escarpments, and do not show a significant development of antithetic faulting. In the eastern part (b), 35°–55° S-dipping normal faults bound the Campo Imperatore plain (a tectonic depression partly filled with alluvial, glacial and fluvioglacial deposits of Quaternary age; Demangeot, 1965), are more segmented than their counterparts in the western part and give rise to more sinuous range fronts. South of these normal faults, between the Campo Imperatore plain and the Middle Aterno Valley, the deformational pattern (c) mainly consist of NE-dipping normal faults, and associated southward tilted fault-blocks determining a morphological aspect given by the close alternation of ridges and depressions (antithetic faults domain, AFD) particularly evident in the shaded relief map of Fig. 3. These NE-dipping faults are antithetic structures in relation to the master faults bounding the Campo Imperatore plain.

2.1. Stratigraphy

The Gran Sasso range is located in the transitional zone between the palaeogeographic domains of the Latium–Abruzzi carbonate platform to the south and the Umbria–Marche pelagic basin to the north (Accordi and Carbone, 1988; Fig. 2). Limestones from the Latium–Abruzzi platform crop out in the main part of the AFD, as far north as the Campo Imperatore plain (Adamoli et al., 1978). The platform-to-basin transition deposits crop out widely north and west of the Campo Imperatore plain along the main topographic elevations of the GSTB. These sediments are well stratified micritic limestones and micritic cherty limestones interbedded with marly and clayey beds, middle Liassic to Middle Miocene in age. This sequence is characterized by strong detrital supply made up of bioclastic limestones, with a pronounced variable thickness, coming from the adjacent Latium–Abruzzi platform. A Messinian flysch ('Flysch della Laga' Formation), representing the siliciclastic infilling of the foredeep basin, crops out only in a few patches in the western part of the Gran Sasso belt. Conversely the Laga Flysch is widespread north of the GSTB, with a thickness of 2–3 km.

Fig. 2. Generalized geologic map of the Gran Sasso range area (modified from Bigi et al., 1990). Legend: *LM* = Laga Mountains; *MFM* = Montagna dei Fiori–Montagnone structure; *CI* = Campo Imperatore plain; *AV* = Assergi Valley; *SS* = S. Stefano Sessanio village; *AFD* = antithetic faults domain; *TV* = Tirino Valley; *MAV* = Middle Aterno Valley.

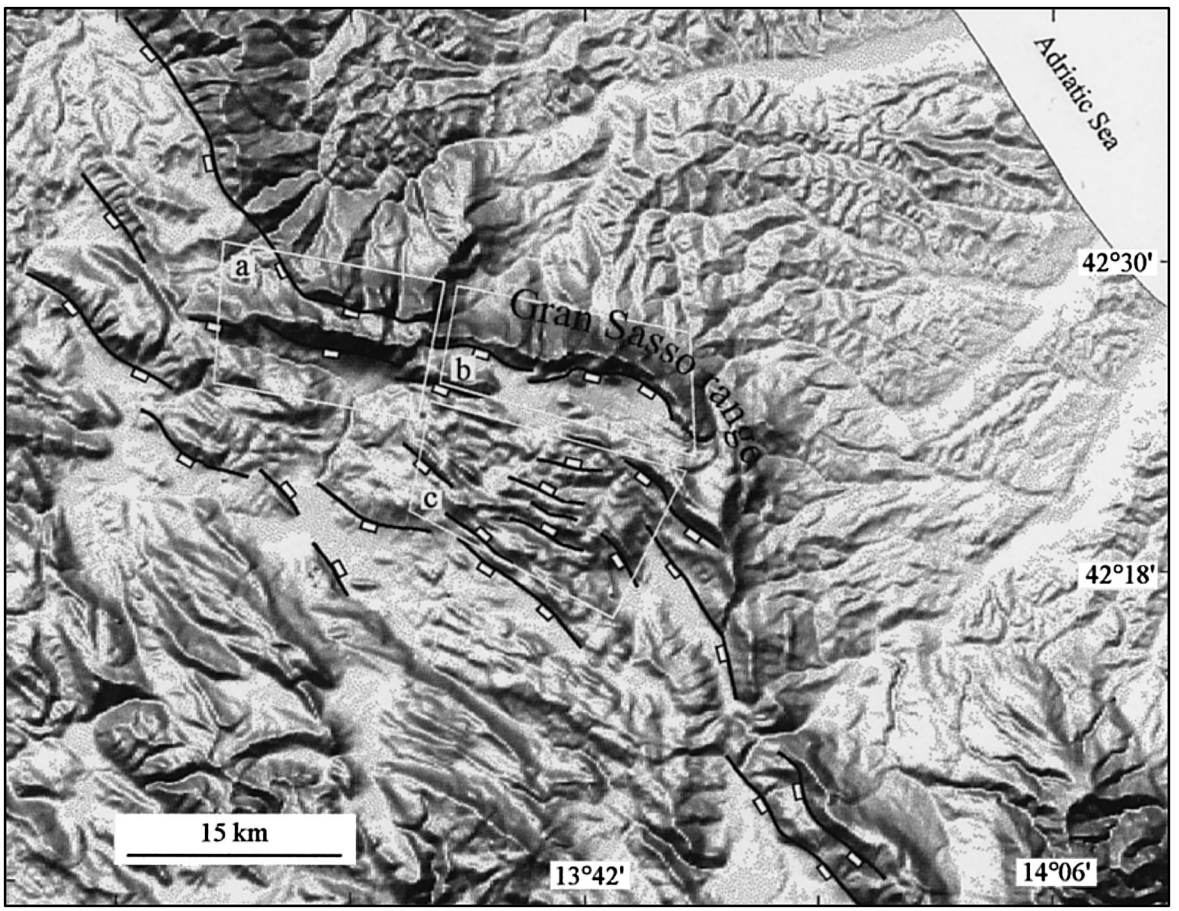

Fig. 3. Shaded relief map of the Gran Sasso range and surrounding areas. Observe the striking morphological expression of the normal faults downthrowing the internal part of the thrust sheet. In the Gran Sasso range the traces of these faults describe a curvature following the arcuate shape of the thrust front. The different extensional domains, distinguished on the basis of structural and morphological features are outlined: (a) western sector; (b) eastern sector; (c) antithetic faults domain, AFD.

Large amounts of Pleistocene detrital deposits can be observed in the area. In the southern part of the range, two different sedimentary sequences have been observed. Lower Pleistocene calcareous conglomerates and breccias (Valle Valiano Breccia, Bosi and Messina, 1991) form the upper part of the alluvial fans bordering the Middle Aterno Valley to the northeast (Fig. 3; Bagnaia et al., 1989; Bertini et al., 1989). Between the Campo Imperatore plain and the Middle Aterno Valley the Quaternary deposits are represented by a pink matrix calcareous breccia, Lower Pleistocene in age ('Brecce mortadella' of Demangeot, 1965; 'Brecce di Fonte Vedice' of Bosi and Messina, 1991; D'Agostino et al., 1997). The 'pink-matrix' breccia generally shows a SSW-dipping direction, having being controlled during their deposition by the NE-dipping faults (see Section 3.3).

2.2. Tectonic setting and pre-existing topography

In the GSTB the E–W-trending structures of the Latium–Abruzzi carbonate platform override the N–S structures of the Montagnone units (Fig. 2; Ghisetti and Vezzani, 1986). Structural (Ghisetti and Vezzani, 1991) and preliminary palaeomagnetic data (Dela Pierre et al., 1992) support an anticlockwise rotation associated with the emplacement of the GSTB, implying a right lateral shear on the N–S-trending segment of the GSTB. In the eastern part of the range (Mt. Prena, Mt. Camicia, Fig. 4A) Ghisetti and

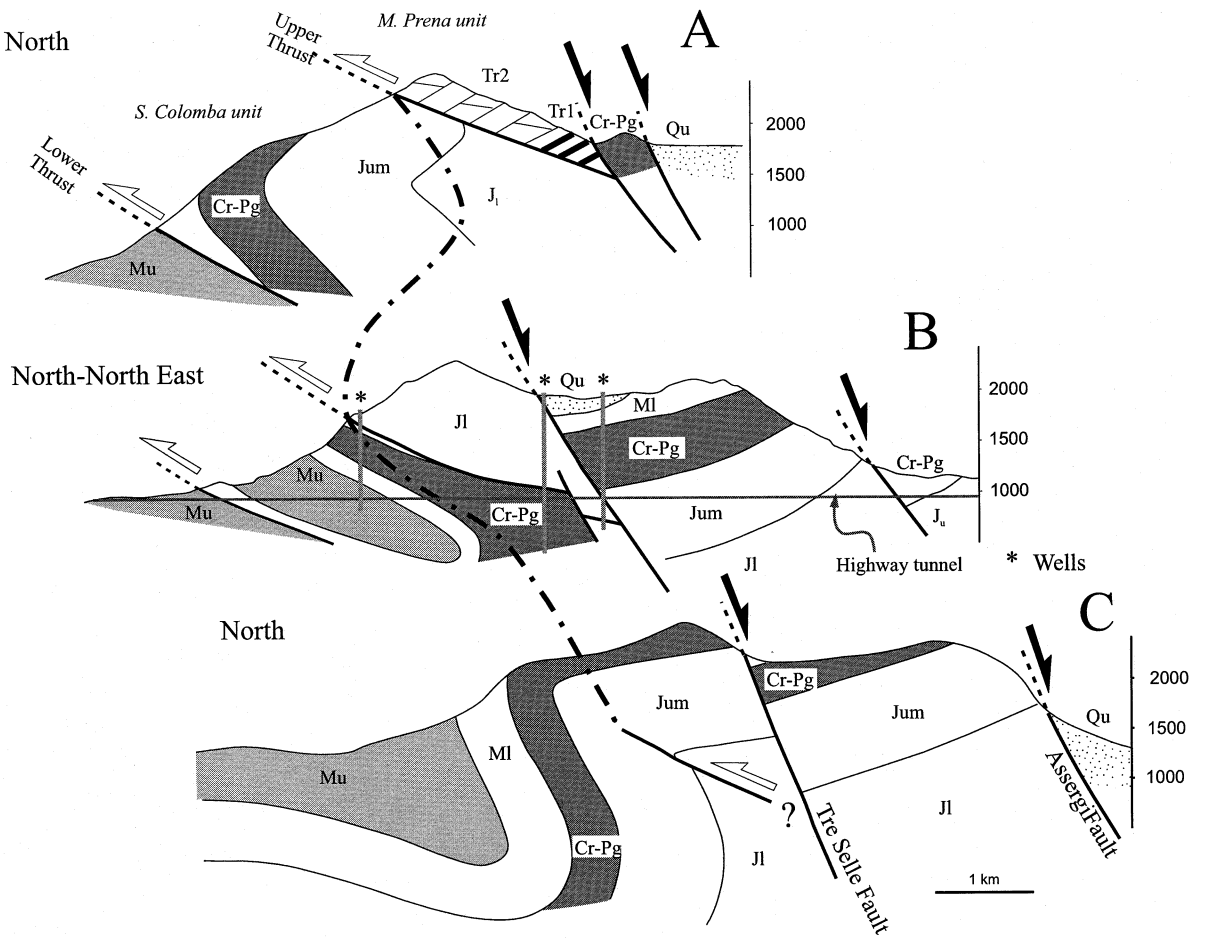

Fig. 4. Cross-sections showing the structural setting of the Gran Sasso thrust belt (see Fig. 2 for location of cross-sections). Observe the decrease in shortening going from the eastern to the western part of the range. (Modified from Servizio Geologico d'Italia, 1963, Ghisetti and Vezzani, 1986, and this work; wells and highway tunnel data from Catalano et al., 1986). Legend: *Tr1* = Upper Trias ('Dolomie bituminose'); *Tr2* = Upper Trias (Dolomia Principale); *Jl* = Lower Jurassic; *Jum* = Upper–Middle Jurassic; *Cr–Pg* = Cretaceous–Palaeogene; *Ml* = Lower Miocene; *Mu* = Upper Miocene; *Qu* = Quaternary.

Vezzani (1986) described an imbricate stack defined by several tectonic units. These units can be differentiated according to their structural setting. The lower unit (S. Colomba unit), overriding the Laga Flysch by means of the Lower Thrust, consists of a Z-shaped folded sequence progressively overturning to the east indicating a west to east increase of shortening (Ghisetti and Vezzani, 1991). The Upper Thrust juxtaposes the Mt. Prena unit, an Upper Triassic–Lower Miocene N-dipping sequence, over the S. Colomba unit. The overlying units, generally made up of N-dipping highly fractured Upper Jurassic to Lower Cretaceous limestones, are separated from the underlying S. Colomba unit by 'younger-on-older' tectonic contacts. Compressional (Ghisetti and Vezzani, 1986, 1991) or extensional (Adamoli et al., 1990; Bally A.W. in Ghisetti et al., 1993; this work) characters have been alternatively proposed for these faults. In the central (Fig. 4B) and in the western part (Fig. 4C), progressively lower shortening is observed. In the westernmost section (Fig. 4C) the front of the thrust belt consists of an overturned anticline, probably related to a blind thrust. The stratigraphic thickness variability along the belt is probably related to both palaeogeographical and tectonic causes (Fig. 4).

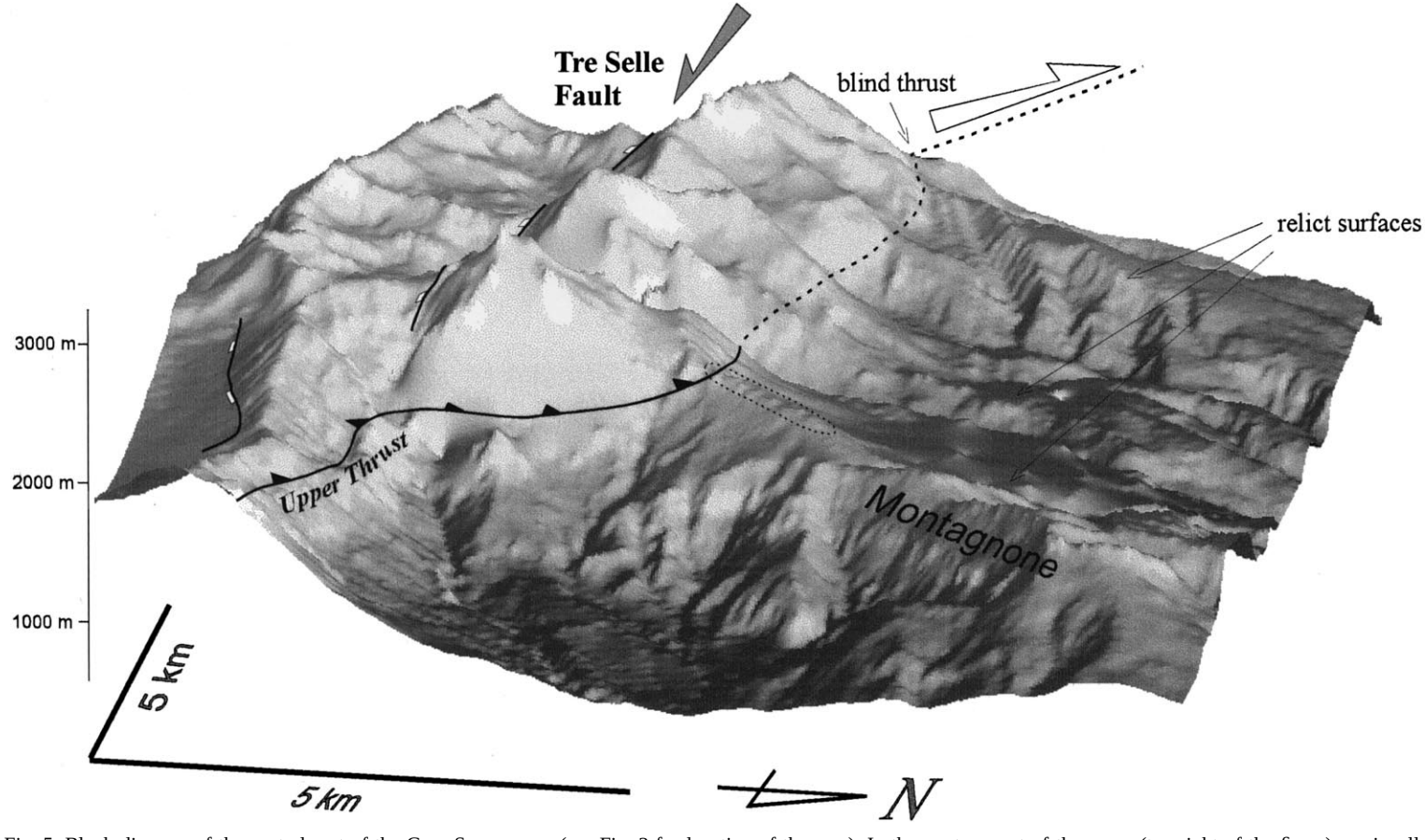

Fig. 5. Block-diagram of the central part of the Gran Sasso range (see Fig. 2 for location of the area). In the western part of the range (top right of the figure) erosionally dissected surfaces, locally preserving thin layers of Lower Pleistocene breccias suturing the thrust front (thin dashed line; Arapietra breccia), allow a first order estimate of the topographic relief formed by thrusting. In the internal part of the range this pre-existing relief has been downthrown to the south by normal faulting.

The emplacement of the Gran Sasso thrust sheet has resulted in the formation of a topographic front that is best preserved, in its original morphology, in the western part of the range (Fig. 5). In this area, after the emplacement of the GSTB, the north-facing slopes underwent mainly linear erosion due to the outflowing Quaternary glaciers and streams. Relict surfaces are preserved 700–900 m lower than the highest elevations and are locally covered by thin layers of Lower Pleistocene breccias (Demangeot, 1965; Dufaure et al., 1988) suturing the thrust front. Considering the elevation of the dissected surfaces and breccia deposits (1900–2000 m) and the elevation of the highest peaks (2600–2800 m), the compressional topographic relief could be evaluated as at least 700–800 m with a mean average slope of 15º. We will show in Section 4.1 how this information can be used to estimate the topographic relief related to normal faulting.

2.3. Timing of normal faulting

The onset of the extensional tectonics in the Gran Sasso area may be inferred by the age of the continental sediments filling intermontane depressions formed after the acme of the compressional episodes. Lower Pleistocene lacustrine sediments (Bosi and Messina, 1991), are widespread in the Middle Aterno Valley, just south of the Gran Sasso range (Fig. 2). These sediments were deposited in an Early Pleistocene lacustrine system, which received considerable detrital supply by the Gran Sasso domain (Bertini et al., 1989). Coarse calcareous conglomeratic bodies are in fact infilled in the Lower Pleistocene lacustrine sequence along the boundary between the Middle Aterno Valley and the Gran Sasso range. In the AFD new magnetostratigraphic data (D'Agostino et al., 1997) have recently confirmed the Lower Pleistocene age of 'pink matrix breccia' (Bosi and Messina, 1991). This seems to demonstrate that both the syn-tectonic deposits in the AFD and the Middle Aterno Valley lacustrine deposits are related to a major extensional pulse during the Early Pleistocene. The observation that the apexes of the Lower Pleistocene alluvial fan deposits of the Middle Aterno Valley depression are cut by northeast-dipping normal faults (Fig. 12), could suggest that, during the Early Pleistocene, the extension shifted towards the northeast affecting progressively the Middle Aterno Valley and the Campo Imperatore area.

3. The extensional faults

3.1. Assergi Valley fault system

The E–W Assergi Valley (Fig. 6) is bounded by a 50º–70º S-dipping normal fault (Assergi Valley fault) with the same orientation. The fault is continuous for more than 10 km, has an offset of more than 1500 m (Servizio Geologico d'Italia, 1963) and limits a ∼1000-m-high escarpment to the north. North of the Assergi Valley the Tre Selle fault (Ghisetti and Vezzani, 1991) trends WNW and extends continuously in the field for more than 10 km. Towards the west, the Tre Selle fault merges with the NW-trending Laga Mts. normal fault (Fig. 3), and cuts the frontal thrust of the GSTB obliquely. The maximum stratigraphic offset of the Tre Selle fault is about 600–700 m (Servizio Geologico d'Italia, 1963). At the bottom of the Maone and Venacquaro valleys, the fault displaces Late Glacial and Holocene deposits and shows well-preserved fault scarps (Fig. 6). Giraudi and Frezzotti (1995), through geomorphic and trenching analysis, inferred at least four seismic events during the last 18,000 years with a slip rate on the fault of 0.67–1 mm/year. The coherence between the Late Glacial–Holocene displacements and the main geological structure suggests that the range-front normal fault grew by repeated similar surface faulting earthquakes (King et al., 1988). The fault dimension and the surface ruptures along the geological structure suggest that this is a major normal fault scaled with the upper seismogenic crust (Jackson and White, 1989). Since the Tre Selle fault shares the same morphological and structural features as the Assergi Valley fault we suggest that they are all major normal faults with a planar high-angle (55º–65º) geometry in the seismogenic layer (10–15 km). The total offset on the Tre Selle fault, assuming a constant slip-rate, is consistent with the beginning of the activity at 600–1000 ka. Since the Assergi Valley fault does not show clear evidence of recent activity and belongs to the same fault system, we suggest that at 600–1000 ka the activity was transferred to the Tre Selle fault.

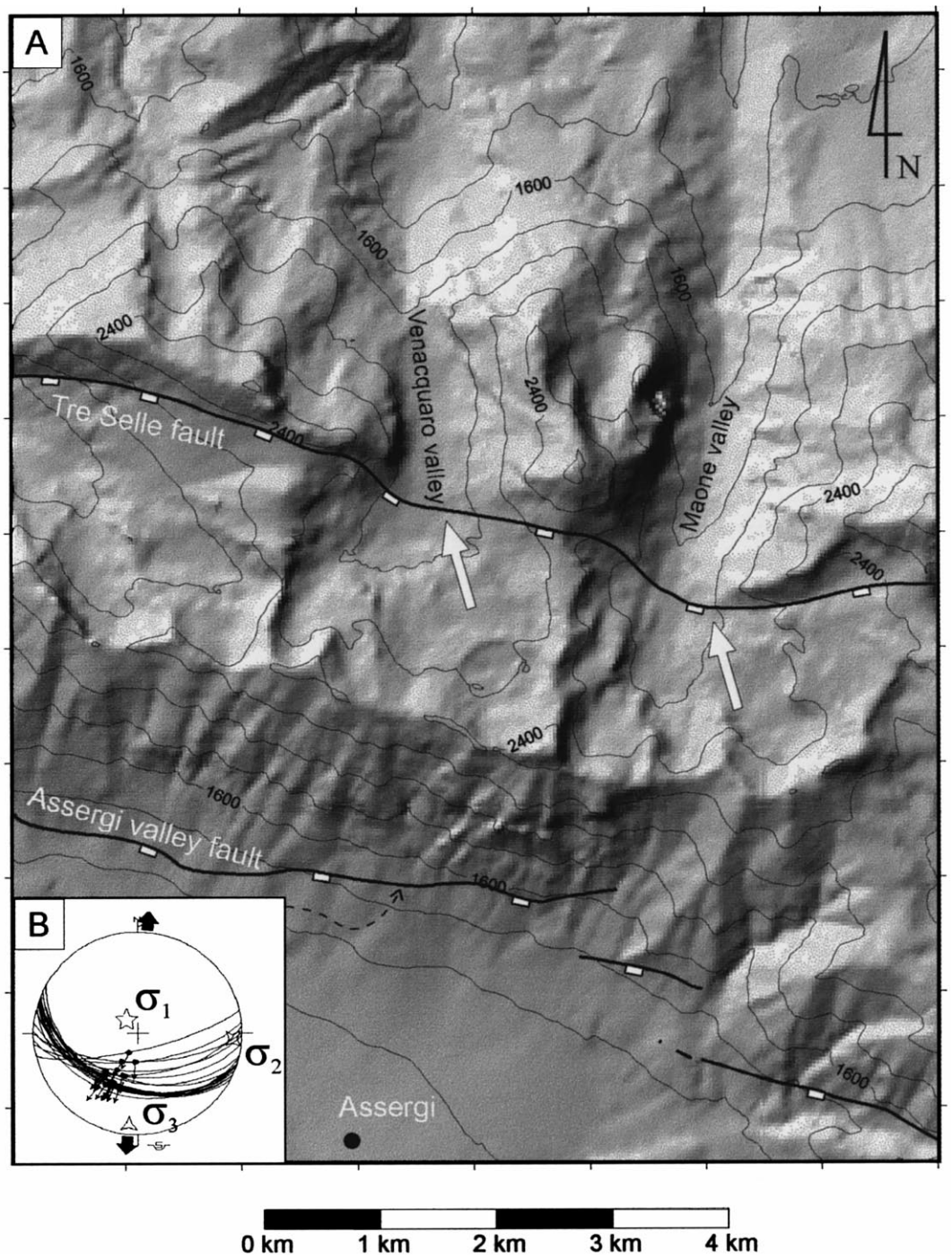

Fig. 6. Assergi Valley and Tre Selle faults (see Fig. 2 for location). (A) Main extensional faults traced on a high-resolution (~40 m) shaded relief map of the western part of the Gran Sasso range. Heavy lines are major range-front normal faults with ticks on down-thrown side. Arrows indicate surface faulting in Late Glacial–Holocene deposits in the Maone and Venacquaro valleys (Giraudi and Frezzotti, 1995). (B) Stereographic plot of fault-slip data collected on the Assergi Valley fault (arrow indicates field site; Schmidt lower hemisphere. The fault slip data sets in this and following figures have been inverted for the palaeo-stress tensor using the method of Angelier, 1984).

3.2. The Campo Imperatore faults

In the Torri di Casanova area (Fig. 7) a well-exposed 25°–30° S-dipping section of the Upper Thrust shows evidence of extensional reactivation. The neo-formed part of the normal fault cuts the hanging wall of the Upper Thrust branching into the 25°–30° dipping fault. S–C structures developed in pelitic horizons both in the hanging wall and in the footwall, indicate top-to-the-south sense of shear, consistent with an extensional reactivation of the thrust. Kinematic indicators on the fault plane confirm that the last deformational event was extensional (Fig. 7C). Field mapping allowed us to accurately trace the reactivated section of the thrust, clearly showing that the upper part (dipping 10°–15°) was not reactivated. In the area, there is no evidence of tilting during the extensional phase (the geometry of the contractional faults does not seem to have been significantly modified) and we thus infer that the extensional movements on the thrust took place on an original low-angle (25°–30°) plane.

At Mt. Camicia, an Upper Triassic–Cretaceous sequence (corresponding to the Mt. Prena unit; Fig. 4) overthrusts the S. Colomba unit and is cut by a south-dipping low (25°–35°) and by high-angle (45°–65°) range-front normal faults (Figs. 8 and 9). A detailed investigation of the kinematic indicators shows that the younger-on-older fault (Mt. Camicia fault) is extensional (Fig. 9). The extensional tectonics evolution in the Mt. Camicia area has been associated with landslide phenomena induced by gravity disequilibrium on the newly created normal fault escarpment. The geometrical relationships between the normal faults, the base of the Verde Ammonitico Formation and the slide surface, allow the reconstruction of the evolution of the normal fault system (Fig. 10). This pattern records the progressive basinward migration of the fault activity as frequently observed around major normal fault systems (Dart et al., 1995).

Two main points stand out from the structural analysis of the Torri di Casanova and Mt. Camicia areas: (1) early extensional faults branch into the Upper Thrust; (2) the Upper Thrust is cut by the later range-front normal faults responsible for the present geometry of the Campo Imperatore plain. We thus suggest that progressively deeper thrusts were reactivated and that the normal faults branching on the Upper Thrust were successively truncated by late normal faults branching on the Lower Thrust.

3.3. The antithetic faults

Detailed field work in the area (D'Agostino et al., 1994; D'Agostino and Tozzi, 1995) has documented NE-dipping rotating normal faults and SW-dipping bedding both in Mesozoic limestones and in the 'pink-matrix' Lower Pleistocene breccias (Figs. 11 and 12). The average dimension of the fault blocks (500 m to 2000 m across strike) and the average fault lengths (from hundreds of metres to a few kilometres) suggest that the fault-blocks are probably detached in shallow upper crustal levels. Two generations of NE-dipping normal faults arranged in a 'domino'-like mode can be observed (Fig. 11). The first set of normal faults dips 20°–40° while the second steeper set of faults is clearly expressed in the morphology, and determines the formation of the closely spaced (1000–2000 m) set of ridges and depressions. The section in Fig. 12a illustrates the deformational pattern of this area and its relationships with the faults bounding the Middle Aterno Valley. A first-order evaluation of the amount of extension can be made assuming a simple 'domino model' (Davison, 1989) constituted by rigid fault blocks rotating around a horizontal axis (Fig. 12b). Even if a precise geometric reconstruction cannot be made, the following should be noted: (1) the association of strongly SW-dipping Mesozoic limestones and two generations of 'domino' normal faults; (2) the near parallelism of breccia and Mesozoic limestones on the southwestern slopes of the rotating fault blocks. These data suggest that most of the deformation in the area occurred in an extensional setting. The amount of extension β is not constant throughout the area and could be evaluated as ranging between 1.25 and 1.75.

4. Tectonic interpretation

4.1. Thin elastic plate model of the Assergi Valley and Tre Selle faults

In order to put further constrain on the geometry of the Assergi Valley and Tre Selle faults we tested

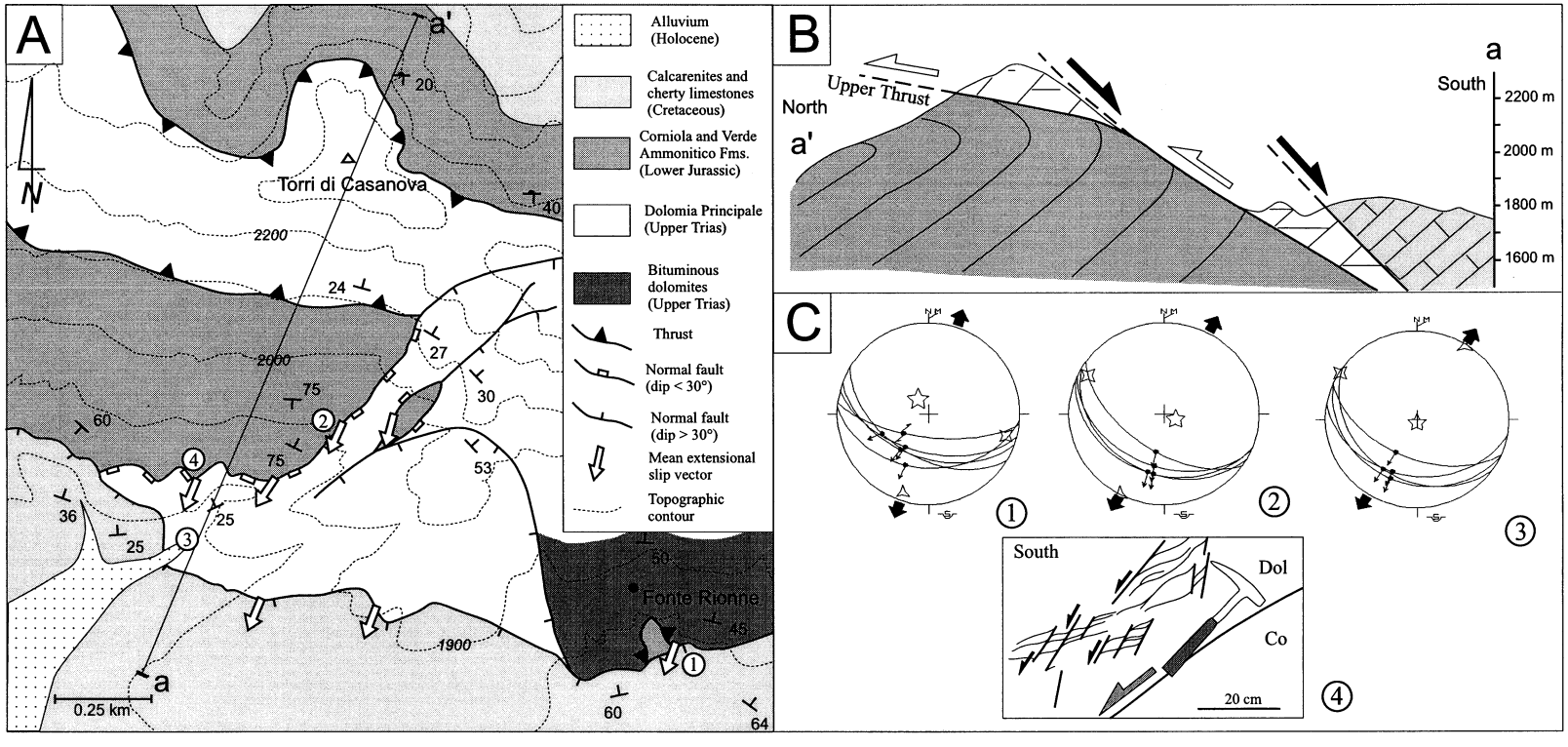

Fig. 7. Geologic map (A) and section (B) of the Torri di Casanova area (location of the area in Fig. 2). The Upper Thrust has been reactivated with extensional movements in its steepest section (25°–30°). In (C) observe the kinematic indicators highlighting the top-to-the-south (extensional) sense of shear on the extensionally reactivated thrust plane. Palaeo-stress axes labels as in Fig. 5.

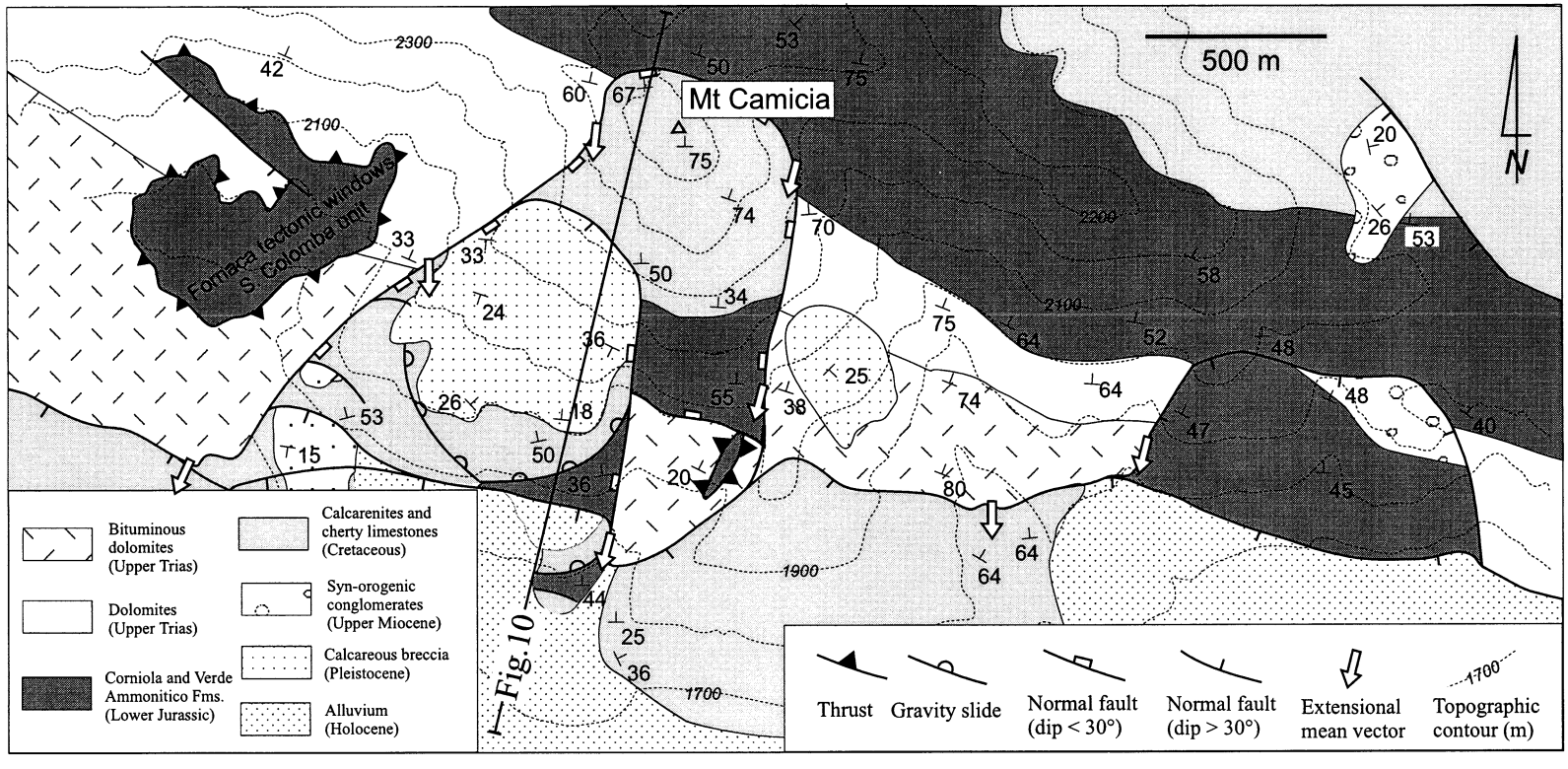

Fig. 8. Geologic map of Mt. Camicia area (location of the area in Fig. 2).

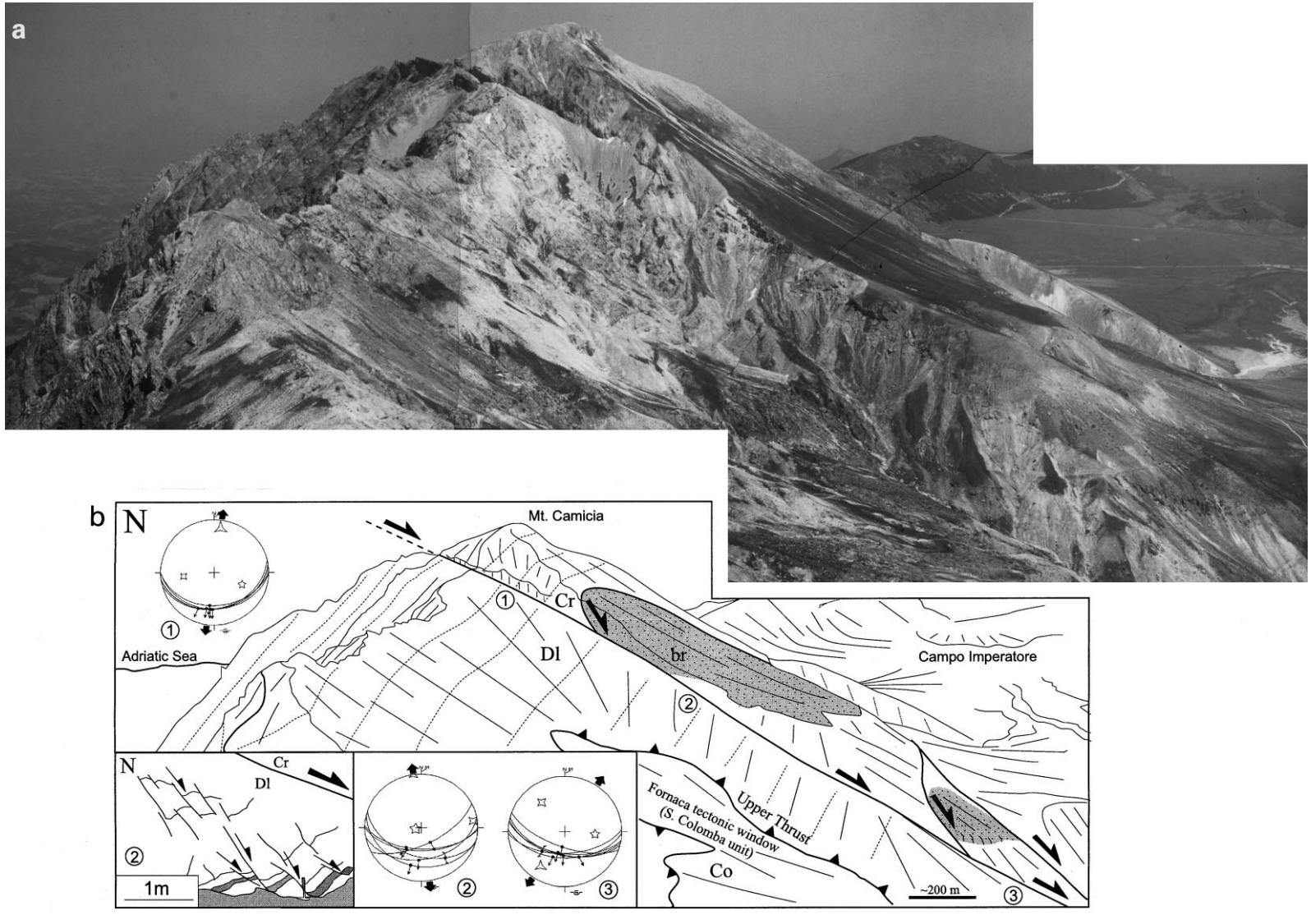

Fig. 9. Mt. Camicia normal fault system: (a) view from the west; (b) tectonic interpretation. The Mt. Camicia normal fault cuts at a low angle (30°–35°) the steeply dipping sequence branching onto the Upper Thrust. On the right side of the photograph, the range-front normal fault cuts both the Mt. Camicia fault and the Upper Thrust (see Fig. 10). Thin dashed lines indicate bedding. Encircled numbers indicate sites where fault-slip data have been collected close to the Mt. Camicia fault (palaeo-stress axes labels as in Fig. 5). Inset sketch of site 2 shows mesoscale extensional structures close to the Mt. Camicia normal fault. *Dl* = Triassic dolomites; *Co* = middle Liassic micritic limestones (Corniola); *Cr* = Cretaceous limestones; *br* = Quaternary breccia.

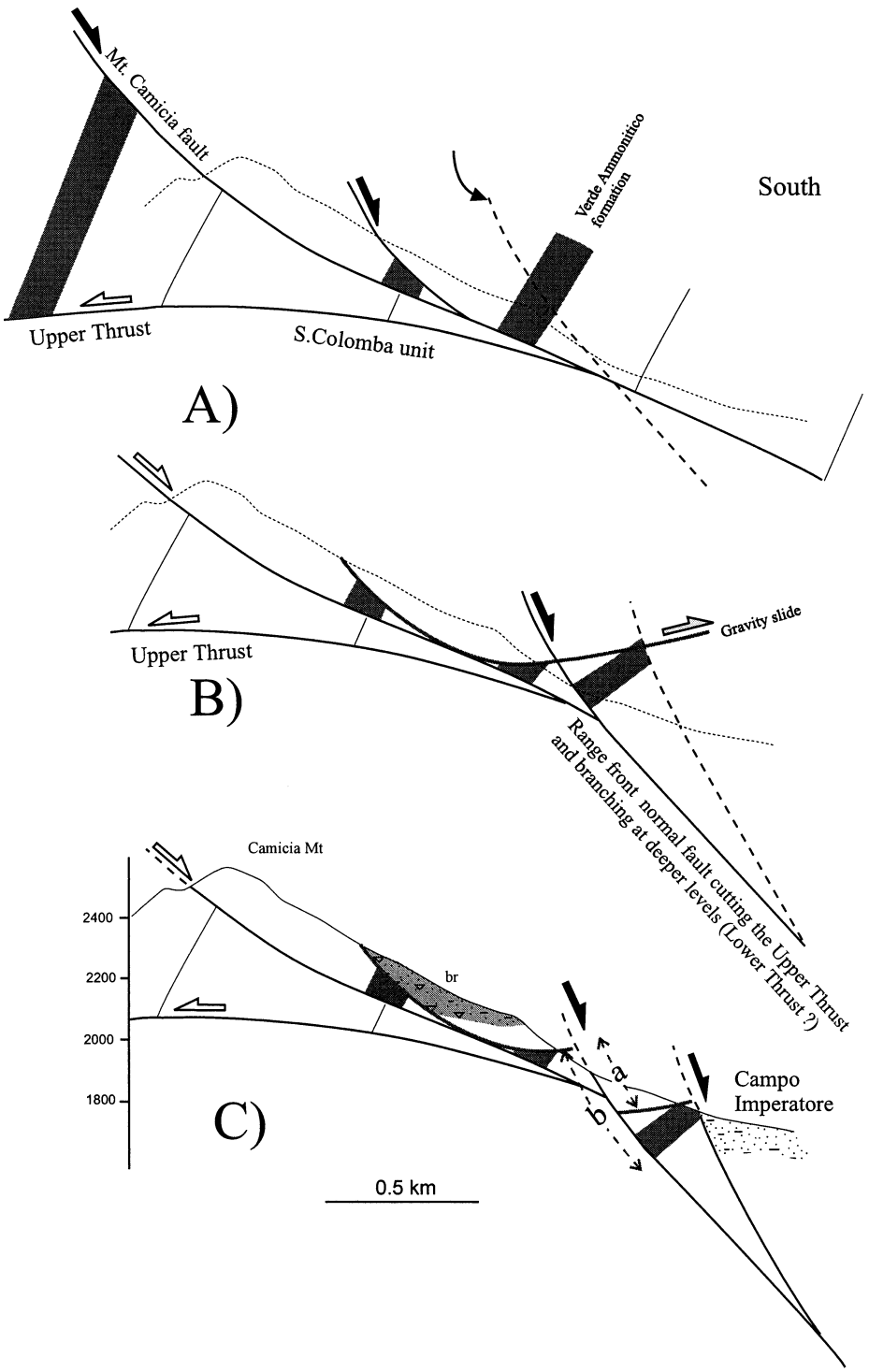

Fig. 10. Geologic reconstruction of the Mt. Camicia fault system (location of the section in Fig. 8). (A) The earlier normal fault (Mt. Camicia fault) soles into the Upper Thrust disrupting the previously overthrust unit. (B) Gravity slide of the escarpment created by later normal faults cutting the Upper Thrust. Note that the gravity slide partly reactivated the Mt. Camicia fault. (C) Present-day structural setting; the different offsets of the slide surface (*a*) and the Verde Ammonitico Formation (*b*) implies that the range-front normal fault has been active before and after the gravity slide.

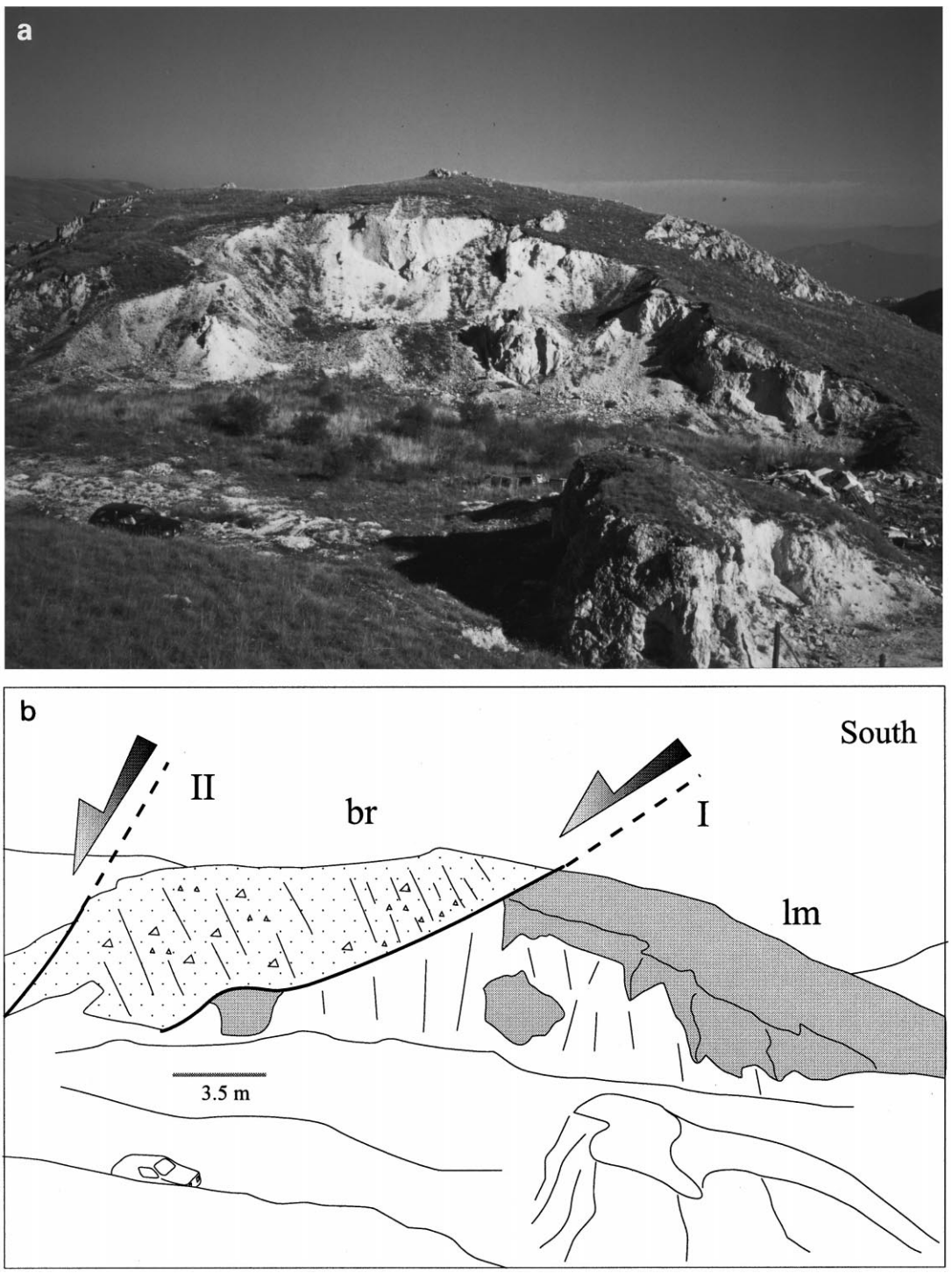

Fig. 11. Domino faulting in the antithetic faults domain (AFD) near S. Stefano Sessanio village. The first generation (*I*) normal fault, juxtaposes Lower Pleistocene 'pink-matrix' breccias (*br*) on Cretaceous limestones (*lm*), and has been rotated to a dip of 25°–30°. The second generation fault (*II*) dips 55°–60° and controlled the formation of a small half-graben to the left of the picture (north).

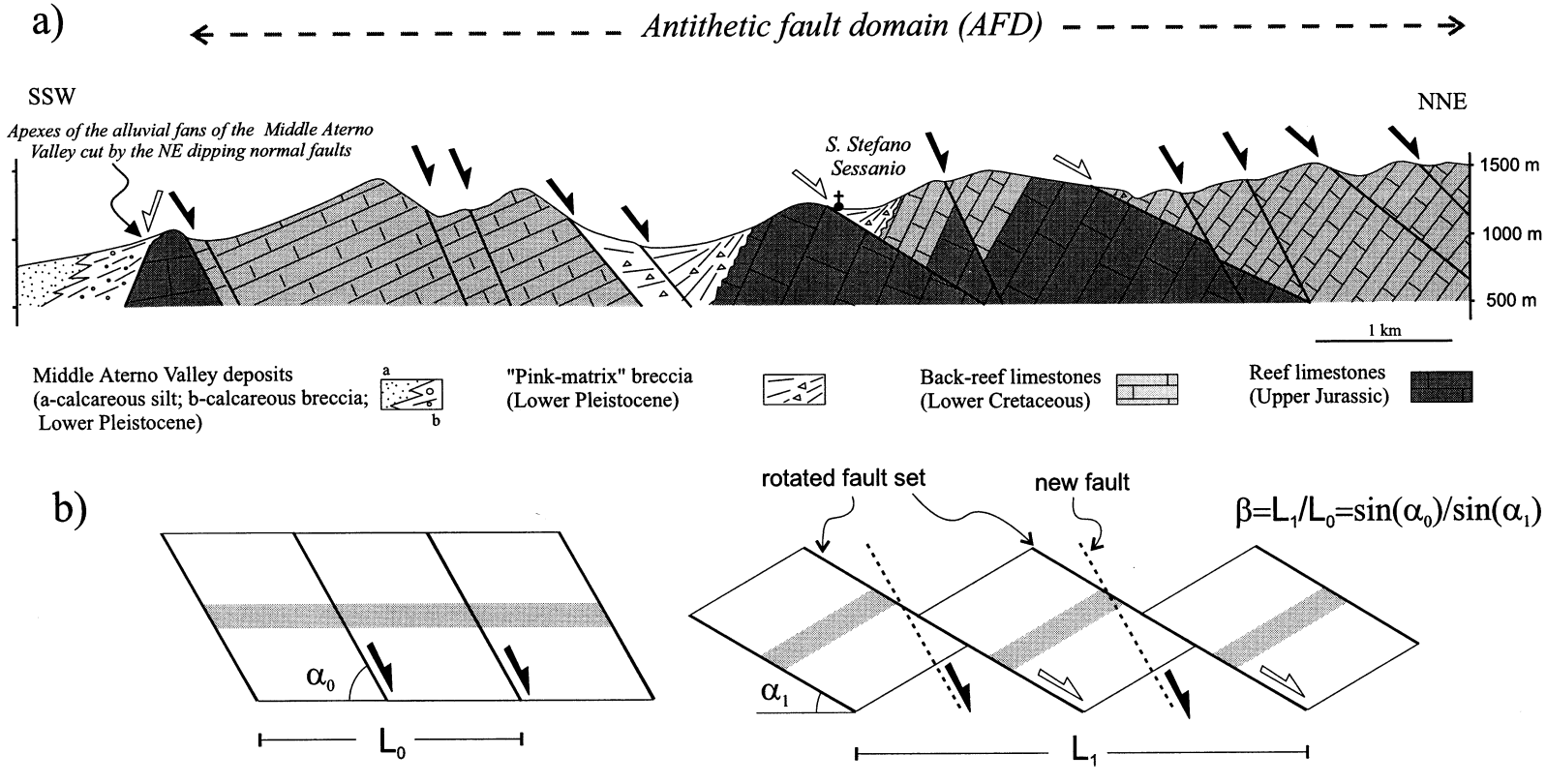

Fig. 12. (a) Geological section of the antithetic faults domain (AFD) (location on Fig. 2). The tectonic style is characterized by NE-dipping rotating normal faults bounding southward-tilted fault blocks. The NE-dipping antithetic faults cut the apexes of the alluvial fans of the Middle Aterno Valley deposits, suggesting that extensional faulting shifted from the Middle Aterno Valley toward the antithetic faults domain (AFD). (b) Domino model adopted to constrain the extension factor β in the AFD. A first-order estimate of the extension may be performed assuming steep initial (60°) fault dip and southwestward tilting of the fault blocks. The geometry of the fault blocks shows that, locally, the extension factor β could be as high as 1.75.

a simple thin elastic plate model (Turcotte and Schubert, 1982) constituted by an elastic layer (equivalent to the seismogenic upper crust) overlying a viscous, fluid layer (equivalent to the lower crust). This model has been previously adopted (Buck, 1988; Weissel and Karner, 1989; Kusznir et al., 1991) to describe the long-term fault behaviour approximating the summation of repeated co-seismic and post-seismic deformation around a major normal fault (King et al., 1988).

The model allows the motion on one or more planar normal faults. The isostatic restoring force is then redistributed regionally using the elastic plate theory. The vertical deflection $w(x)$ of the thin plate is calculated by solving the following differential equation:

$$D\frac{\mathrm{d}^4 w(x)}{\mathrm{d}x^4} + \Delta\rho w(x) = p(x) \tag{1}$$

where D is the flexural rigidity related to the elastic plate thickness (T_e) by:

$$D = \frac{T_e^3 E}{12(1-\nu^2)} \tag{2}$$

where Young's modulus $E = 2.5e10$ N/m^2 and Poisson's ratio $\nu = 0.25$. The other parameters, assuming isostatic compensation in the lower crust, are $\Delta\rho = 2.85$ g cm^{-3} (density difference between the underlying fluid-like medium and the infilling material), $g = 9.81$ m s^{-2} and $p(x)$, the isostatic loads. The final geometry is therefore the sum of the 'kinematic' depression (motion on planar faults) and the regionally deflected thin plate. The deflection of the thin plate is calculated by the superposition of the effects of linear point-loads on a continuous infinite plate (Turcotte and Schubert, 1982). In Fig. 13 we calculated the elevation (normalized to the displacement) for a 60°-dipping planar normal fault for various values of elastic thickness. As already

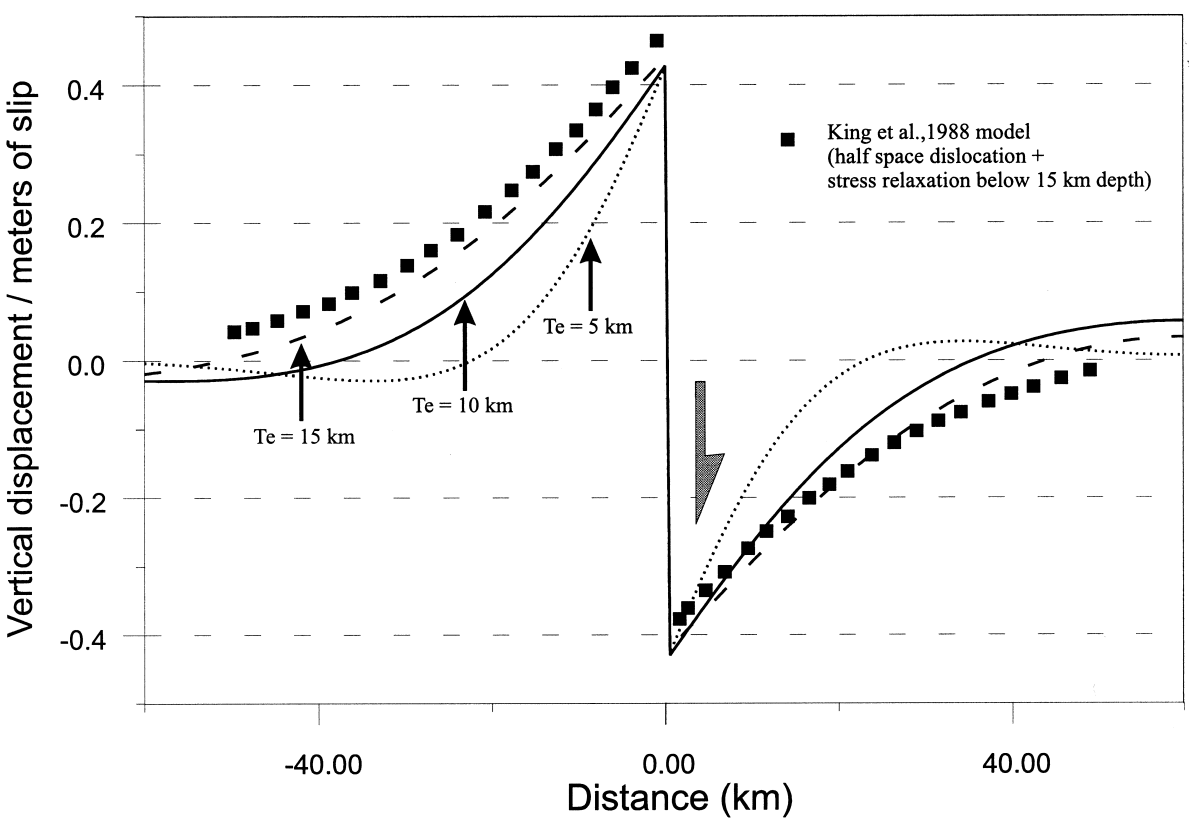

Fig. 13. Flexural modelling of normal fault (dip 60°) for increasing elastic thickness (*Te*) and comparison with an elastic dislocation model with total stress relaxation below 15 km (from King et al., 1988). The two kinds of model present very similar across-strike patterns of uplift and subsidence.

pointed out by King et al. (1988), the uplift and subsidence normal to the fault strike is controlled by the mechanical properties of the upper crust, the structure being wider for larger flexural rigidities. Stein et al. (1988) modelled several dip-slip geological structures and found that the best-fitting elastic thickness was in the 2–4 km range. This is significantly lower than the thickness of seismogenic crust implying that the long-term behaviour of the upper crust is represented by a significantly lower mechanical thickness (King et al., 1988; Buck, 1988; Armijo et al., 1996). Fig. 13 also shows the agreement between the thin-plate model calculations compared with the results of King et al. (1988) based on an half-space dislocation model with stress relaxation in the lower crust.

In Fig. 14 we searched for the best-fit solution for a topographic section crossing the Assergi Valley and Tre Selle faults. We first evaluated the contribution of the pre-existent topography. In Section 2.2 we estimated the pre-existing relief of the thrust belt. This simplified topography can be removed from the present-day topography to obtain the relief related to normal faulting (Fig. 14). The fault dips and offsets have been constrained from the existing geologic data (Servizio Geologico d'Italia, 1963) and field mapping. The resultant topography (Fig. 14) has been satisfactorily modelled by a 2-km-thick elastic plate. This value is consistent with the results found by Stein et al. (1988). Our value of elastic thickness is in the lower end of their elastic thickness range possibly because of the highly fractured upper crust following the Neogene compressional tectonics.

We believe that this model, despite the masking effects of the pre-existing topography on the true flexural profile, can account for the isostatic response of a high-angle planar normal fault cutting through the upper crust. The results support the preliminary interpretation, made on the basis of structural and morphological features, that in the westernmost portion of the GSTB the Quaternary extension has been accommodated on high-angle normal faults in the upper crust.

4.2. Kinematic evolution and geometry of the Campo Imperatore faults and the antithetic faults

The geological reconstruction of the Mt. Camicia normal fault system, traced in Fig. 10, can be mechanically explained considering the evolution of the lithostatic load on the fault surfaces. The decrease of the lithostatic load, as a result of continuing movement and unloading on the earlier normal faults, forces a downward shift of the reactivated low-angle fault from the Upper Thrust to the Lower Thrust. This hypothesis is in accordance with the Mohr–Coulomb criterion analysis of Huyghe and Mugnier (1992) who pointed out the progressive deepening of the potential thrust reactivation in extensional settings undergoing progressive exhumation. It is interesting to note that the Mt. Camicia normal fault, probably branching onto the Upper Thrust in its non-exposed part, assumes a similar dip approaching the thrust fault (Figs. 9 and 10). This geometrical pattern has also been observed in analogue models and has been explained as the influence of a pre-existing weak zone on the local stress field (Faccenna et al., 1995).

The development of the antithetic faults appears to be genetically related to the Campo Imperatore faults. A simple geometrical model (King et al., 1985; Groshong, 1989; Daniel, 1994) can be used to explain the development of antithetic faulting on a major normal fault system made of a steep section branching on a low-angle reactivated fault (Fig. 15). This model assumes that the offset (*R*) along the high-angle fault is entirely transferred to the low-dipping reactivated section, causing antithetic faulting in the hanging wall. Fig. 15b shows the geometrical and mathematical relations between *Rh* and *Eh*, the component of motion along the steep and the low-dipping section, respectively. The ratio between *Eh* and *Rh* represents moreover the extensional factor β_a in the antithetic domain plotted in Fig. 15c for various geometries. The model considers an homogeneously deforming antithetic domain. We think that this simplification is justified considering the small average spacing of the antithetic faults in relation to the whole deformed area.

Geological observations constrain α and θ to have the same value in the range 55°–65 and β_a to range between 1.25–1.75. The model provides dip values for the low-angle fault between 10°–50°. Considering that the Lower Thrust should be at a shallow upper crustal level beneath the AFD we believe that its reactivation could explain the main features of the extensional style in the eastern GSTB. A value

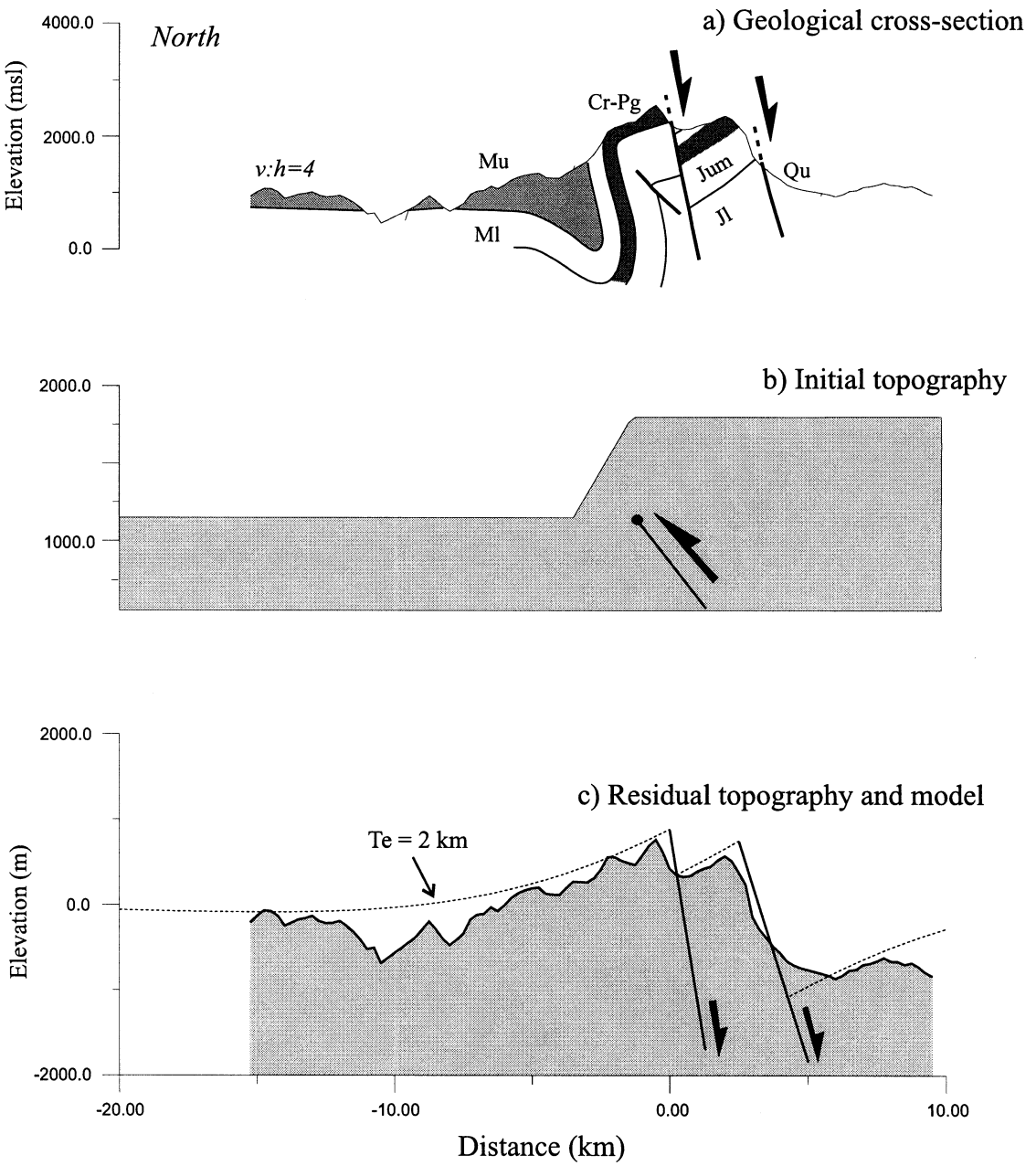

Fig. 14. Thin elastic plate flexural modelling of the Assergi Valley and Tre Selle faults. (a) Geological cross-section across the Tre Selle and Assergi faults (trace of the section and legend as in Fig. 4C). (b) Reconstructed initial topography related to the compressional emplacement of the GSTB. (c) Flexural modelling of the residual topography (present-day minus initial topography).

of 30°–35° for the reactivated part of the Lower Thrust is consistent with: (1) field observations in the Campo Imperatore area (Figs. 7 and 9); (2) geometrical models of fault reactivation (Fig. 15); (3) mechanical models based on the Mohr–Coulomb criterion (Sibson, 1985).

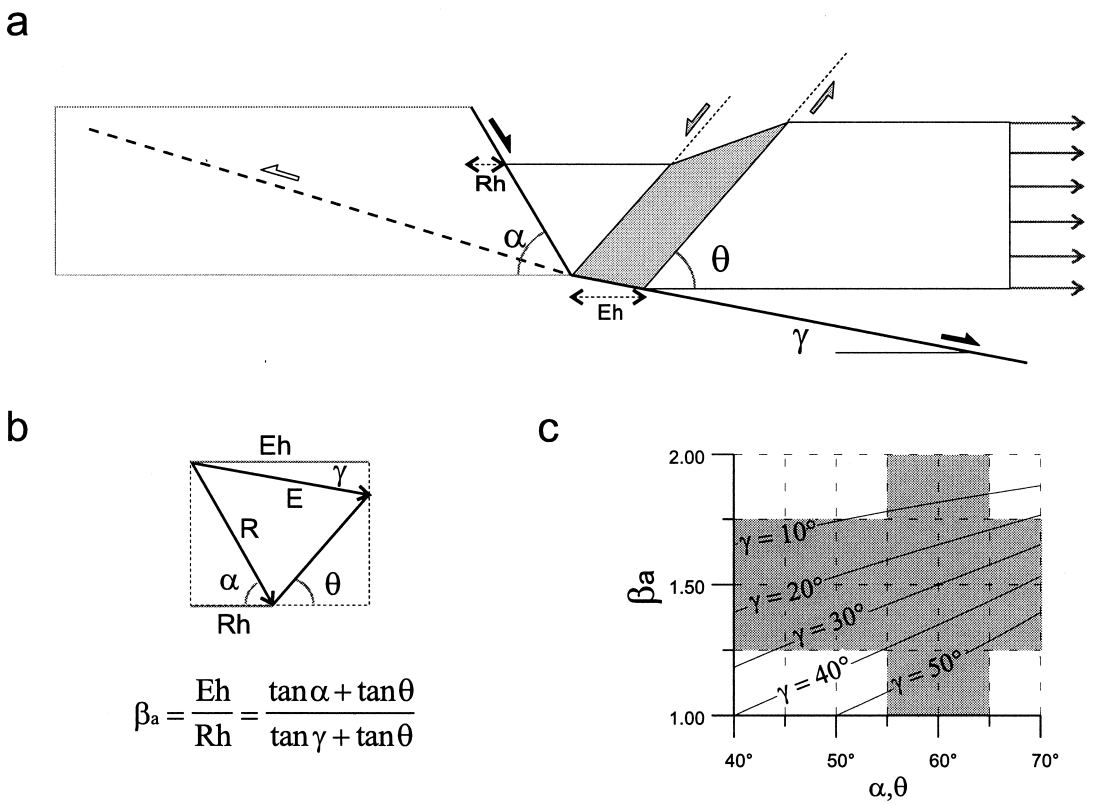

Fig. 15. Geometric model for the development of antithetic faulting around steep normal fault branching on a low-angle section; (a) geometric elements; (b) vector plot; and (c) relationship between dip of master and antithetic shear and extensional factor β_a in the antithetic domain. Considering $\alpha = \theta = 55^o$ to 65^o and $\beta_a = 1.25$ to 1.75, the value of γ range between 10^o and 50^o.

5. Discussion

5.1. Extensional styles in the Gran Sasso range and the migration of deformation

In the western Gran Sasso range, extension is accommodated by high-angle normal faults, cutting through the entire upper crustal brittle layer including older thrusts. Conversely, the eastern part of the belt is characterized by a ramp-flat geometry of extensional faults and the related antithetic deformation is confined above the extensionally reactivated Lower Thrust (Fig. 16). The timing of normal faulting shows that the entire Gran Sasso area is in extension since the Early Pleistocene. The different styles of extension, between the eastern and western parts, thus contemporaneously developed during the Quaternary extensional tectonic episodes.

The geometrical setting of the external limit of the Apennines extensional domain provides insight into the modes of eastward migration of normal faulting in the central Apennines. Between the Laga Mountains and Sulmona plain (Figs. 2 and 3) the NW-trending external limit of normal faulting describes an arcuate pattern following the compressional structures of the GSTB. The proposed anti-clockwise thrust-sheet emplacement of the GSTB accounts for a higher topographic relief and more developed weak zones in the eastern part of the range. Kinematics data on normal faults show a component of right lateral oblique slip on the E–W normal faults (Figs. 6, 7 and 9). This suggests that the development of the E–W normal faulting is consistent with the NE–SW regional extension and could have been controlled by: (1) reactivation of pre-existing surfaces (e.g. Campo Imperatore faults); (2) the perturbation of the local stress regime induced by pre-existing topographic contrast. We infer that both processes operated be-

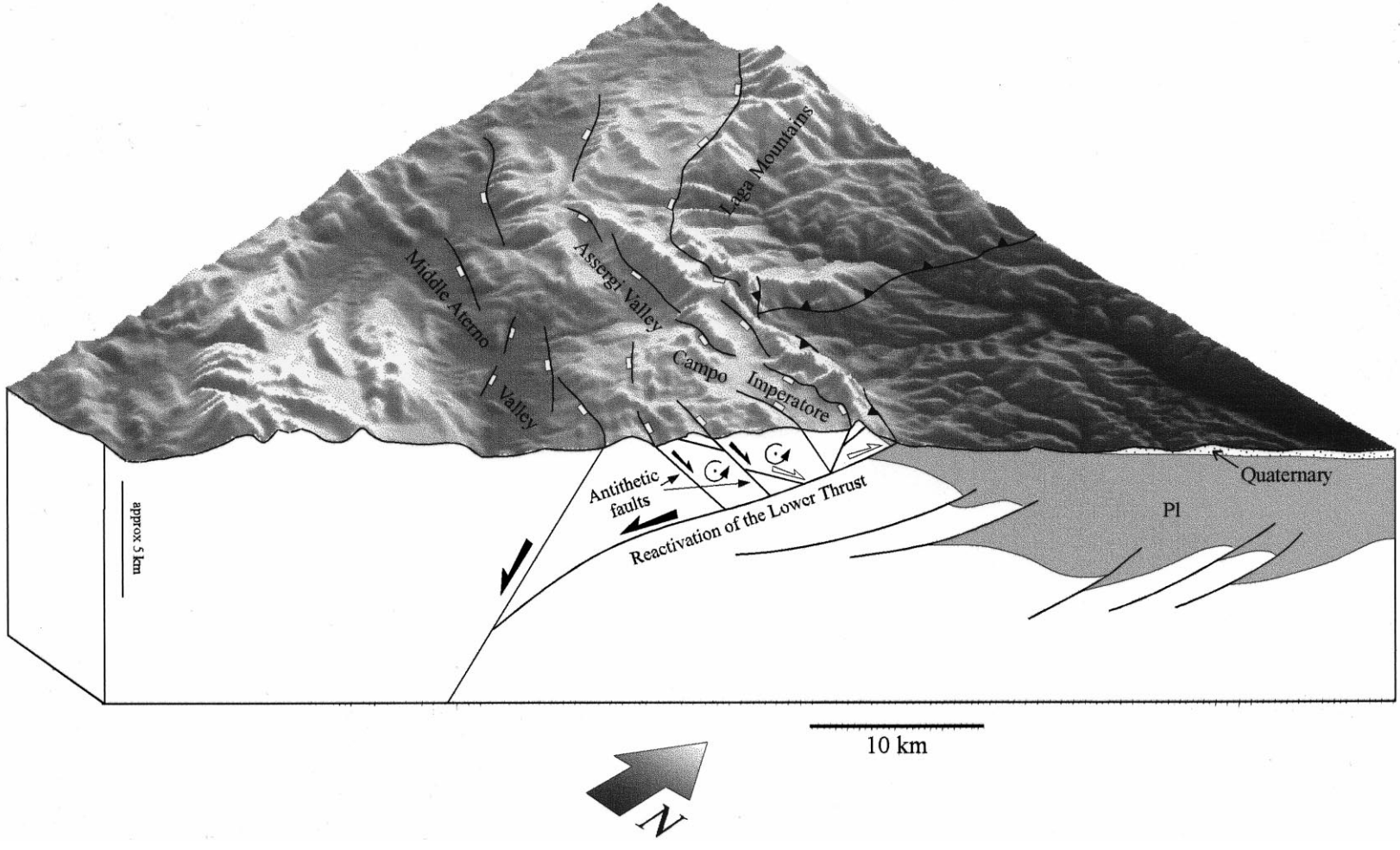

Fig. 16. Block-diagram of the Gran Sasso range area. The schematic cross-section shows structural setting in the eastern part of the range (Campo Imperatore plain and antithetic faults domain). The Lower Thrust has been extensionally reactivated causing the downthrowing and deformation on antithetic faults in the internal part of the thrust sheet. In this area extension and block-tilting are confined in the hanging wall of this major extensional fault system.

cause high-angle and low-angle normal faults cut and reactivated, respectively, compressional structures. Stress fields arising from topographic reliefs as volcanic constructs (van Wyk de Vries and Merle, 1996) were shown to interact with the regional extensional stress field. The same mechanism may have operated in the Gran Sasso area, where the migrating regional NW–SE-trending limit of normal faulting interacted with the relief and pre-existing structures constituting the GSTB, determining the higher northeastern advance of normal faulting with respect to the surrounding regions (Fig. 3).

5.2. Upper crust normal faults geometry and the influence of a pre-existing tectonic setting

In comparison to the eastern Gran Sasso extensional style (Figs. 6, 8 and 11) in well-studied major normal fault systems (e.g. Gulf of Corinth; King et al., 1985; Armijo et al., 1996; Rigo et al., 1996), antithetic faulting generally accommodates less of the overall extension. It is possibly the depth at which normal faults assume a shallower dip which controls the extent of antithetic faulting. In the case of a high-angle normal fault detaching at the base of the upper crust (as in the Corinth rift; Rigo et al., 1996) hanging-wall deformation could be partly accommodated at the base of the brittle layer, thus reducing deformation by antithetic faulting. For a normal fault branching on an upper crust low-angle discontinuity all the hanging-wall deformation is accommodated mostly through the formation of antithetic faults. Diffuse brecciation or the presence of soft layers (as in the case of the Upper Miocene deposits overthrust by the GSTB) could provide a zone of mechanical decoupling in the upper crust allowing block tilting of several tens of degrees.

Seismological observations on the largest earthquakes in central Italy (Anderson and Jackson, 1987; Westaway et al., 1989) have shown that active deformation is accommodated by steep planar normal faults in the upper 10–15 km of the crust as usually observed in extensional settings (Jackson and White, 1989). Below this depth, it is generally considered that the high-angle normal faults (rupturing during seismic events) assume shallower dips rooting into the ductile lower crust (Eydogan and Jackson, 1985; Rigo et al., 1996). This work shows that a major shallowing in normal fault geometry is possible in the upper crust as a result of the reactivation of pre-existing thrust faults.

In highly extended terrains, much debate has focused on the initial geometries of the present-day very low-angle detachment faults. Buck (1988) and Brun et al. (1994), through thin elastic plate and analogue modelling, respectively, proposed that both isostatic restoring forces and very low flexural rigidities could contribute to rotation of initial high-angle normal faults to very shallow-dipping ($<30^{o}$) detachment. Nevertheless there is considerable evidence that some low-angle normal faults originated and have been active with their present-day geometry (e.g. Hodges et al., 1989). The fact that low-angle normal faults exist in an area with a minimal amount of structural exposure indicates that these geometries are not exclusive of highly extended terrains and that normal faults could originate either with a low- or high-angle geometry according to the pre-existing tectonic setting. Since many active intracontinental extensional settings follow orogenic areas, the reactivation of pre-existing gently dipping discontinuities could substantially contribute to the process of crustal extension.

5.3. Regional-scale topography and extensional tectonics

In the Apennines significant normal faulting begins immediately behind the topographic crest (Fig. 1b). This feature is shared with other extended domains (see Roy et al., 1996) where extension has been associated with uplift and has deeply affected regional morphology. Several authors have presented evidence for the Quaternary uplift of central Italy from the Tyrrhenian to the Adriatic coast (Ambrosetti et al., 1982; Dufaure et al., 1988; Marinelli et al., 1993) across an area more than 150 km wide. This long-wavelength regional uplift has interacted with the shorter-wavelength normal faulting processes. This interaction is evident in the topographic profiles (Fig. 1b) where the relief is composed of a major long-wavelength topographic bulge ($\sim$150 km wide) and a shorter wavelength ($\sim$30 km) determined mostly by normal faulting. This suggests that the Quaternary regional-scale morphological evolution has been controlled by the contempora-

neous eastward migration of the long-wavelength topographic bulge and the short-wavelength normal faulting. This last process has progressively downthrown toward the southwest parts of the uplifting accretionary complex.

6. Conclusion

The Quaternary styles of extension in the Gran Sasso range seem to depend on pre-existing tectonic and topographic settings. In the western part of the range where previous tectonic shortening was less severe, long, range-front normal faults cut at a high angle through the brittle upper crust. Conversely, in the eastern sector, characterized by greater previous tectonic shortening, the normal faults reactivated progressively deeper pre-existing 30º–35º-dipping thrust faults. The branching of the upper high-angle part of normal faults onto the thrust faults determined the formation of second-order antithetic 'domino' faulting confined in the hanging-wall of the extensional fault system. This work shows that gently dipping (25º–35º) normal faults could be active in the upper crust as a consequence of reactivation of older thrusts. The process of reactivation of pre-existing thrust faults could be a mechanism for the development of low-angle normal faults in moderately extended terrains in post-orogenic extensional settings. The fault pattern in the Gran Sasso area indicates that the pre-existing topographic relief has influenced the geometry of the migrating limit of normal faulting, causing a major northeastern advance with respect to the surrounding areas.

Acknowledgements

The authors wish to thank Sveva Corrado, Claudio Faccenna, Massimo Mattei and Fabrizio Storti for useful comments and critical reviews of the manuscript. Thoughtful reviews by Mary Ford and Jaume Vergés helped to improve the manuscript. Figs. 1, 5 and 16 were produced with GMT software (Wessel and Smith, 1995). This work has been supported by a MURST 40% grant ('Tettonofisica e geodinamica della litosfera') for the year 1995.

References

Accordi, G., Carbone, F. (Eds.), 1988. Carta delle litofacies del lazio-Abruzzo ed aree limitrofe. Consiglio Nazionale delle Ricerche P.G.F., Quad. Ric. Sci. 114 (5).

Adamoli, L., Bertini, L., Chiocchini, M., Deiana, G., Mancinelli, A., Pieruccini, U., Romano, A., 1978. Ricerche geologiche sul Gran sasso d'Italia (Abruzzo), II. Evoluzione tettonico sedimentaria dal Trias superiore al Cretaceo inferiore dell'area compresa tra il Corno Grande e S. Stefano di Sessanio (F.140 Teramo). Stud. Geol. Camerti 4, 7–18.

Adamoli, L., Bigozzi, A., Ciarapica, G., Cirilli, S., Passeri, L., Romano, A., Duranti, F., Venturi, F., 1990. Upper Triassic bituminous facies and Hettangian pelagic facies in the Gran Sasso range. Boll. Soc. Geol. Ital. 109, 219–230.

Ambrosetti, P., Carraro, F., Deiana G., Dramis, F., 1982. Il sollevamento dell'Italia Centrale tra il Pleistocene inferiore e il Pleistocene medio. Consiglio Nazionale delle Ricerche P.G.F., Pubbl. 513, pp. 219–223.

Anderson, H., Jackson, J.A., 1987. Active tectonics of the Adriatic region. Geophys. J. R. Astron. Soc. 91, 937–983.

Angelier, J., 1984. Tectonic analysis of faults slip data sets. J. Geophys. Res. 89, 5835–5848.

Armijo, R., Meyer, B., King, G.C.P., Rigo, A., Papanastassiou, D., 1996. Quaternary evolution of the Corinth Rift and its implications for the Late Cenozoic evolution of the Aegean. Geophys. J. Int. 126, 11–53.

Bagnaia, R., D'Epifanio, A., Sylos Labini, S., 1989. Aquila and Subequan basins: an example of quaternary evolution in the Central Apennines, Italy. Quat. Nova 1, 1–23.

Bally, A.W., Burbi, L., Cooper, C., Ghelardoni, R., 1986. Balanced cross sections and seismic reflection profiles across the Central Apennines. Mem. Soc. Geol. Ital. 35, 257–310.

Bally, A.W., Gordy, P.L., Stewart, P.A., 1966. Structure, seismic data and orogenic evolution of the Southern Canadian Rochy Mountains. Bull. Can. Pet. Geol. 14, 337–381.

Bertini, T., Bosi, C., Galadini, F., 1989. La conca di Fossa–S. Demetrio dei Vestini. In: Elementi di tettonica pliocenico–quaternaria ed indizi di sismicità olocenica nell'Appennino laziale-abruzzese. Guida all'escursione della Società Geologica Italiana.

Bigi, G., Cosentino, D., Parotto, M., Sartori, R., Scandone, P., 1990. Structural model of Italy and gravity map. Consiglio Nazionale delle Ricerche P.G.F., Quad. Ric. Sci. 114 (3).

Bosi, C., Messina, P., 1991. Ipotesi di correlazione fra successioni morfo-litostratigrafiche plio–pleistoceniche nell'Appennino laziale–abruzzese. Stud. Geol. Camerti 2, 257–263.

Brun, J.P., Sokoutis, D., Van Den Driessche, J., 1994. Analogue modelling of detachment fault systems and core complexes. Geology 22, 319–322.

Buck, R.W., 1988. Flexural rotation of normal faults. Tectonics 7, 959–973.

Catalano, P.G., Cavinato, G.P., Salvini, F., Tozzi, M., 1986. Analisi strutturale nei laboratori dell'INFN del Gran Sasso d'Italia. Mem. Soc. Geol. Ital. 35, 647–655.

D'Agostino, N., Speranza, F., Funiciello, R., 1997. Le Brecce

Mortadella dell'Appennino Centrale: primi risultati di stratigrafia magnetica. Quaternario 10 (2).
D'Agostino, N., Tozzi, M., 1995. Rotazione di blocchi su assi orizzontali al margine meridionale del massiccio del Gran Sasso. Stud. Geol. Camerti 2, 183–189.
D'Agostino, N., Funiciello, R., Speranza, F., Tozzi, M., 1994. Caratteri della tettonica distensiva nell'Appennino Centrale: l'area di S. Stefano Sessanio–Calascio (l'Aquila). Boll. Soc. Geol. Ital. 113, 37–53.
Daniel, J.M., 1994. Thèse de Doctorat, Université Pierre et Marie Curie, Paris.
Dart, C., Cohen, H.A., Akyuz, H.S., Barka, A., 1995. Basinward migration of rift-border faults: implications for facies distributions and preservation potential. Geology 23, 69–72.
Davison, I., 1989. Extensional domino fault tectonics: kinematics and geometrical constraints. Ann. Tectonicae 3, 12–24.
Dela Pierre, F., Ghisetti, F., Lanza, R., Vezzani, L., 1992. Paleomagnetic and structural evidence of neogenic tectonic rotation of the Gran Sasso range (Central Apennines, Italy). Tectonophysics 215, 335–348.
Demangeot, J., 1965. Gèomorphologie des Abruzzes Adriatiques. Centre Recherche et Documentation Cartographiques Memoires et Documents, Numero hors serie, 403 pp.
Doser, D.I., 1987. The Ancash, Peru, earthquake of 1946 November 10: evidence for low-angle normal faulting in the high Andes of northern Peru. Geophys. J.R. Astron. Soc. 91, 57–71.
Dufaure, J.J., Bossuyt, D., Rasse, M., 1988. Déformations quaternaires et morphogénèse de l'Apennin Central adriatique. Physio-Géo 18, 9–46.
Elter, P., Giglia, G., Tongiorgi, M., Trevisan, L., 1975. Tensional and compressional areas in the recent (Tortonian to present) evolution of North Apennines. Boll. Geofis. Teoret. Appl. 17, 3–18.
Eydogan, H., Jackson, J., 1985. A seismological study of normal faulting in the Demirci, Alasehir and Gediz earthquakes of 1969–70 in western Turkey: implications for the nature and geometry of deformation in the continental crust. Geophys. J.R. Astron. Soc. 81, 569–607.
Faccenna, C., Nalpas, T., Brun, J.P., Davy, P., 1995. The influence of pre-existing thrust faults on normal fault geometry in nature and in experiments. J. Struct. Geol. 17, 1139–1149.
Fleitout, L., Froidevaux, C., 1982. Tectonics and topography for a lithosphere containing density heterogeneities. Tectonics 1, 21–56.
Ghisetti, F., Vezzani, L., 1986. Assetto geometrico ed evoluzione strutturale della catena del Gran sasso tra Vado di Siella e Vado di Corno. Boll. Soc. Geol. Ital. 105, 131–171.
Ghisetti, F., Vezzani, L., 1991. Thrust belt development in the Central Apennine (Italy): northward polarity of thrusting and out-of-sequence deformations in the Gran Sasso chain. Tectonics 10, 904–919.
Ghisetti, F., Barchi, M., Bally, A.W., Moretti, I., Vezzani, L., 1993. Conflicting balanced structural section across the Central Apennines (Italy): problems and implications. In: Spencer, A.M. (Ed.), Generation, Accumulation and Production of Europe's Hydrocarbon, III. Spec. Publ. Eur. Assoc. Pet. Geol. 3, 219–231.
Giraudi, C., Frezzotti, F., 1995. Paleoseismicity in the Gran Sasso massif (Abruzzo, Central Italy). Quat. Int. 25, 81–93.
Groshong, R.H., 1989. Half-graben structures: balanced models of extensional fault-bend folds. Geol. Soc. Am. Bull. 101, 96–105.
Hodges, K.V., McKenna, L.W., Stock, J., Knapp, J., Page, L., Sternlof, K., Silverberg, D., Wust, G., Walker, J.D., 1989. Evolution of extensional basin and range topography west of Death Valley, California. Tectonics 8, 453–467.
Huyghe, P., Mugnier, J.L., 1992. The influence of depth on reactivation in normal faulting. J. Struct. Geol. 14, 991–998.
Ivins, E.R., Dixon, T.H., Golombek, M.P., 1990. Extensional reactivation of abandoned thrust: a bound on shallowing in the brittle regime. J. Struct. Geol. 12, 303–314.
Jackson, J., White, N., 1989. Normal faulting in the upper continental crust: observations from regions of active extension. J. Struct. Geol. 11, 15–36.
Keller, J.V.A., Minellii, G., Pialli, G., 1994. Anatomy of late orogenic extension: the Northern Apennines case. Tectonophysics 238, 275–294.
King, G.C.P., Ouyang, Z.K., Papadimitriou, P., Deschamps, A., Gagnepain, J., Housemann, G., Jackson, J.A., Soufleris, C., Virieux, J., 1985. The evolution of the Gulf of Corinth (Greece): an aftershock study of the 1981 earthquakes. Geophys. J.R. Astron. Soc. 80, 677–693.
King, G.C.P., Stein, R.S., Rundle, J.B., 1988. The growth of geological structures by repeated earthquakes, 1. Conceptual framework. J. Geophys. Res. 93, 13307–13318.
Kusznir, N.J., Marsden, G., Egan, S.S., 1991. A flexural-cantilever simple-shear/pure shear model of continental lithosphere extension: application to the Jeanne d'Arc Basin, Grand Banks and Viking Graben, North Sea. In: Roberts, A.M., Yelding, G., Freeman, B. (Eds.), The Geometry of Normal Faults. Geol. Soc. Spec. Publ. 56, 41–60.
Malinverno, A., Ryan, W.B., 1986. Extension in the Tyrrhenian Sea and shortening in the Apennines as a result of arc migration driven by sinking of the lithosphere. Tectonics 5, 227–246.
Marinelli, G., Barberi, F., Cioni, R., 1993. Sollevamenti neogenici e intrusioni acide della Toscana e del Lazio settentrionale. Mem. Soc. Geol. Ital. 49, 279–288.
Parotto, M., Praturlon, A., 1975. Geological Summary of the Central Apennines. In: Structural Model of Italy. C.N.R., Quad. Ric. Sci. 90, 257–311.
Patacca, E., Sartori, R., Scandone, P., 1990. Tyrrhenian basin and Apenninic arcs: kinematic relations since late Tortonian times. Mem. Soc. Geol. Ital. 45, 425–451.
Petersen, T.D., Brown, L.D., Cook, F.A., Kufman, S., Oliver, J.E., 1984. Structure of the Riddleville basin from COCORP seismic data and implications for reactivation tectonics. J. Geol. 92, 261–271.
Powell, C.M., Williams, G.D., 1989. The Lewis/Rocky Mountains trench fault system in Northwest Montana, USA: an example of negative inversion tectonics? In: Cooper, M.A.,

Williams, G.D. (Eds.), Inversion Tectonics. Geol. Soc. Spec. Publ. 44, 223–234.

Rigo, A., Lyon-Caen, H., Armijo, R., Deschamps, A., Hatzfeld, D., Makropoulos, K., Papadimitriou, P., Kassaras, I., 1996. A microseismic study in the western part of the Gulf of Corinth (Greece): implications for large-scale normal faulting mechanisms. Geophys. J. Int. 126, 663–688.

Roy, M., Royden, L.H., Burchfiel, B.C., Tzankov, T., Nankov, R., 1996. Flexural uplift of the Stara Planina range. Basin Res. 8, 143–156.

Royden, L.H., Burchfiel, B.C., 1987. Thin skinned N–S extension within the convergent Himalayan region: gravitational collapse of a miocene topographic front. In: Coward, M.P., Dewey, J.F., Hancock, P.L. (Eds.), Continental Extensional Tectonics. Geol. Soc. Spec. Publ. 28, 611–619.

Royse, F., Jr., Warner, M.A., Reese, D.L., 1975. Thrust belt structural geometry and related stratigraphic problems Wyoming–Idaho–northern Utah. In: Bolyard, D.W. (Ed.), Symposium on Deep Drilling Frontiers in the Central Rocky Mountains, Stemboats Springs, CO. Rocky Mountain Association of Geologists, pp. 41–54.

Servizio Geologico d'Italia, 1963. Carta geologica d'Italia, Foglio n. 140. Teramo, Roma.

Sibson, R.H., 1985. A note on fault reactivation. J. Struct. Geol. 7, 751–754.

Smith, R.B., Bruhn, R.L., 1984. Intraplate extensional tectonics of the Eastern Basin-Range: inferences on structural style from seismic reflection data, regional tectonics, and thermal–mechanical models of brittle–ductile deformation. J. Geophys. Res. 89, 5733–5762.

Stein, R.S., King, G.C.P., Rundle, J.B., 1988. The growth of geological structures by repeated earthquakes, 2. Field examples of continental dip-slip faults. J. Geophys. Res. 95, 13319–13331.

Turcotte, D.L., Schubert, G., 1982. Geodynamics: Applications of Continuum Physics to Geological Problems. John Wiley, New York.

van Wyk de Vries, B., Merle, O., 1996. The effect of volcanic constructs on rift fault patterns. Geology 24, 643–646.

Wessel, P., Smith, W.H.F., 1995. New version of the Generic Mapping Tools released. EOS, Trans. Am. Geophys. Union 76, 329.

Weissel, J.K., Karner, G.D., 1989. Flexural uplift of rift flanks due to mechanical unloading of the lithosphere during extension. J. Geophys. Res. 94, 13919–13950.

Wernicke, B., Walker, J.D., Beaufait, M.S., 1985. Structural discordance between Neogene detachments and frontal Sevier thrusts, Central Mormon Mountains, Southern Nevada. Tectonics 4, 213–246.

Westaway, R., Gawthorpe, R., Tozzi, M., 1989. Seismological and field observations of the 1984 Lazio–Abruzzo earthquakes: implications for the active tectonics of Italy. Geophys. J. Int. 98, 489–514.